Planetary and Space Science 155 (2018) 50–72

Contents lists available at ScienceDirect

Planetary and Space Science

journal homepage: www.elsevier.com/locate/pss

Titan's cold case files - Outstanding questions after Cassini-Huygens

C.A. Nixon [a,*], R.D. Lorenz [b], R.K. Achterberg [c], A. Buch [d], P. Coll [e], R.N. Clark [f], R. Courtin [g], A. Hayes [h], L. Iess [i], R.E. Johnson [j], R.M.C. Lopes [k], M. Mastrogiuseppe [l], K. Mandt [b], D.G. Mitchell [b], F. Raulin [e], A.M. Rymer [b], H. Todd Smith [b], A. Solomonidou [k,m], C. Sotin [k], D. Strobel [n], E.P. Turtle [b], V. Vuitton [o], R.A. West [j], R.V. Yelle [p]

[a] Planetary Systems Laboratory, NASA Goddard Space Flight Center, Greenbelt, MD 20771, USA
[b] Johns Hopkins Applied Physics Laboratory, Laurel, MD 20723, USA
[c] Department of Astronomy, University of Maryland, College Park, MD 20742, USA
[d] LGPM, LGPM, CentraleSupelec, Gif-sur-Yvette, France
[e] LISA, UPEC-UPD/CNRS/IPSL, Paris-Créteil, France
[f] Planetary Science Institute, Tucson, AZ 85719, USA
[g] LEISA, Observatoire de Paris, 92195 Meudon Cedex, France
[h] Astronomy Department, Cornell University, Ithaca, NY 14853, USA
[i] Dipartimento di Ingegneria Meccanica e Aerospaziale, Università La Sapienza, via Eudossiana 18, 00184 Rome, Italy
[j] Department of Materials Science and Engineering, University of Virginia, Charlottesville, VA 22904, USA
[k] Jet Propulsion Laboratory, California Inst. of Technology, 4800 Oak Grove Drive, Pasadena, CA 91109, USA
[l] Department of Information, Electronical and Telecommunications Engineering, University La Sapienza, Rome, Italy
[m] European Space Agency (ESA), European Space Astronomy Centre (ESAC), Madrid, Spain
[n] Earth and Planetary Sciences, Johns Hopkins University, Baltimore, MD 21218, USA
[o] University of Grenoble Alpes, CNRS, IPAG, F-38000 Grenoble, France
[p] Lunar and Planetary Laboratory, University of Arizona, Tucson, AZ, USA

A B S T R A C T

The entry of the Cassini-Huygens spacecraft into orbit around Saturn in July 2004 marked the start of a golden era in the exploration of Titan, Saturn's giant moon. During the Prime Mission (2004–2008), ground-breaking discoveries were made by the Cassini orbiter including the equatorial dune fields (flyby T3, 2005), northern lakes and seas (T16, 2006), and the large positive and negative ions (T16 & T18, 2006), to name a few. In 2005 the Huygens probe descended through Titan's atmosphere, taking the first close-up pictures of the surface, including large networks of dendritic channels leading to a dried-up seabed, and also obtaining detailed profiles of temperature and gas composition during the atmospheric descent. The discoveries continued through the Equinox Mission (2008–2010) and Solstice Mission (2010–2017) totaling 127 targeted flybys of Titan in all. Now at the end of the mission, we are able to look back on the high-level scientific questions from the start of the mission, and assess the progress that has been made towards answering these. At the same time, new scientific questions regarding Titan have emerged from the discoveries that have been made. In this paper we review a cross-section of important scientific questions that remain partially or completely unanswered, ranging from Titan's deep interior to the exosphere. Our intention is to help formulate the science goals for the next generation of planetary missions to Titan, and to stimulate new experimental, observational and theoretical investigations in the interim.

1. Introduction

On October 10th–11th 2016, as Cassini entered the final year of its 13-year mission at Saturn, a mini-workshop was convened entitled "Titan: Cold Case Files" during a meeting of the Cassini Project Science Group (PSG) in Monrovia, CA. Scientists in attendance collectively took the opportunity to review and reflect on the accomplishments of Cassini and Huygens with regard to Titan science, considering topics such as: has Cassini-Huygens answered all the questions that we set out to address at the start of the mission? If we were unable to answer some questions, what would it take to answer them in future? And finally, what new questions in Titan science have arisen during the mission?

Some cases were indeed closed: the issue of whether Titan has widespread surface hydrocarbon oceans is 'no', while localized seas were discovered at the north pole (Stofan et al., 2007). The existence of an interior ocean is considered a robust 'yes' at this point, following the measurement of Titan's deformation under Saturn's gravity (Bills and Nimmo, 2008, 2011; Iess et al., 2012). A perplexing mystery of specular

* Corresponding author.
E-mail address: conor.a.nixon@nasa.gov (C.A. Nixon).

https://doi.org/10.1016/j.pss.2018.02.009
Received 5 August 2017; Received in revised form 13 January 2018; Accepted 16 February 2018
Available online 21 February 2018

reflection from discrete locations on Titan's surface during a bistatic RADAR experiment in the early 2000s (Campbell et al., 2003) has just recently been resolved, showing that dry lake/sea beds – not liquids - at locations now known as Hotei and Tui Regios, were the culprits (Hofgartner et al., in preparation). Unanticipated motions of the Huygens probe are now explained (Lorenz, 2017) and Titan's rotational oscillation periods were found to be in excellent agreement with model predictions (Bills and Nimmo, 2011).

However, the list of unanswered questions was longer. Some of these, such as the pathways to formation of Titan's haze and whether Titan is active, remain from the Voyager 1 flyby, were key questions at the start of the mission (Matson et al., 2002; Lebreton and Matson, 2002), and remain almost as mysterious today. Other topics are new, such as whether the shorelines of lakes and seas discovered in 2006 (Stofan et al., 2007) are changing (Hayes et al., 2011) and what is the composition of these liquid bodies (Cordier et al., 2012); while in the atmosphere we search for an explanation for Titan's hydrogen gradient (Strobel, 2010), and whether methane is hydrodynamically escaping from the exobase (Strobel, 2008; Yelle et al., 2008).

Following the workshop, it was decided to collect the proceedings into a review article – resulting in this paper. Herein, we focus only on the current status of the unanswered questions, since excellent descriptions of the 'closed cases' are already to be found in the literature, along with books and review articles describing Titan science from Cassini-Huygens. Our purpose here is to summarize in one place some of the key Titan science questions remaining for the next generation of missions and scientists, a particularly important and exciting aspect of Cassini's legacy.

The paper begins with open questions surrounding Titan's history (Section 2) moving on to unresolved issues regarding the interior and surface (Section 3), lower and middle atmosphere (Section 4), and finally upper atmosphere and exosphere (Section 5). In Section 6 we consider how these questions might be addressed by future missions, laboratory experiments and theoretical investigations.

2. Titan's history

2.1. The sources and sinks of Titan's methane

Long before Cassini-Huygens, the origin and persistence of Titan's atmospheric methane was already a mystery. It was realized in the early 1970s that methane is irreversibly converted to C_2 and heavier hydrocarbon species, as a result of photolysis (Strobel, 1974). Models in the wake of the Voyager 1 encounter in 1980, which provided the first detailed picture of the atmospheric composition, computed that the present methane amount would be destroyed in a timescale of just ~10 Myr – less than 1% of the age of the solar system - unless resupplied to the atmosphere (Yung et al., 1984). A related problem was the fate of methane photochemical products – primarily ethane. Over geologic time, this should have accumulated to a sizable kilometer-deep global ethane ocean (Strobel, 1982; Lunine et al., 1983; Flasar, 1983; Yung et al., 1984). A major goal of the Cassini-Huygens investigation at Titan was to address these twin problems of the 'sources' and 'sinks' of Titan's methane. The question of the 'sinks' has proved somewhat tractable, the 'sources' less so.

Considering first the 'sinks': in contrast to the expected global ethane ocean or substantial seas, Cassini found only much smaller liquid hydrocarbon seas (Stofan et al., 2007), enough to account for 75,000 years of photochemistry (Sotin et al., 2012), which appear in any case to be of primarily methane composition (Section 3.5). A more substantial surface hydrocarbon deposit is the planet-girdling dune field (Lorenz et al., 2006a,b), sufficient to account for several 100s of Myr of carbon accumulation (Sotin et al., 2012), but still far short of the solar system age. In addition, this solid material does not allow us to account for ethane liquid. An alternative hypothesis advanced by Choukroun and Sotin (2012) is that ethane rain seeps into the crust and supplants methane from clathrate cages. This mechanism simultaneously allows for 50% recycling of carbon atoms (one methane released for one ethane retained) and also provides an explanation for Titan's shape figure, as the 300 m difference in equator to polar radius could be explained by the heavier ethane clathrate causing polar subsidence in a timescale of 300–1200 Myr.

Fig. 1 shows that currently we can at best account for around 10% of the heavy carbon production that would have occurred over the age of the solar system: either we have missed some deposits (perhaps the mid-latitude 'blandlands', or seepage into the interior), or else methane depletion has been less in the past.

Primary sources of methane supply at the present day such as cryovolcanism have been diligently sought in Cassini data, but with scant and inconclusive evidence from visible, infrared (IR) and RADAR imaging (Section 3.2). Another possibility is that methane seeps from the crust into a sub-surface methane 'table', linked to the bases of the seas (Hayes et al., 2008), which then buffer the atmosphere through evaporation. Circumstantial evidence for interior outgassing comes from the detection of ^{40}Ar, a radiogenic decay product of ^{40}K that was detected at significant amounts by the Huygens Gas Chromatograph and Mass Spectrometer (GCMS) (4×10^{-5}, Niemann et al., 2005). However, this ^{40}Ar may equally have come from a single outburst which supplied the entire atmospheric methane inventory some ~600 Myr ago in a crustal destabilization event (Tobie et al., 2006), with no subsequent geologic activity. This leaves the question of present day resupply of methane to the atmosphere entirely open, with the implication that it could all vanish in several tens of Myr. If that were to occur, Titan's atmosphere could

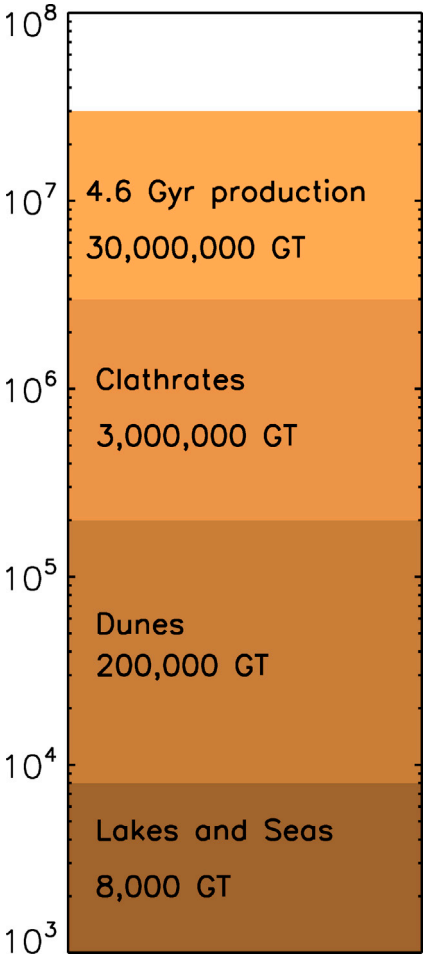

Fig. 1. Carbon budget for Titan's surface: lakes and seas (Sotin et al., 2012); dunes (Le Gall et al., 2011); polar clathrate deposits (Choukroun and Sotin, 2012) and carbon deposits expected over 4.6 Gyr (Sotin et al., 2012), assuming today's methane depletion rates held in past.

collapse (Lorenz et al., 1997) and enter a new 'snowball' phase (Wong et al., 2015).

Answering questions about the sources and sinks of Titan's methane remains a major goal for future missions to address:

- Was methane captured into Titan's interior, or formed later?
- What is the relative balance of methane resupply/destruction, and is there a net positive or negative flux into the atmosphere from the interior at the present day?
- Has Titan's atmosphere collapsed in the past, or will it in the future (Lorenz et al., 1997)?
- Is ethane being largely sequestered into Titan's crust?
- What proportion of carbon becomes solid material (dunes) versus liquid (ethane)?

One means of probing methane's history is through precise measurement of the isotopic composition via spectroscopy or in situ sampling, since photochemical processes can induce changes in the isotopic composition over time through the kinetic isotope effect (Mandt et al., 2012; Nixon et al., 2012).

2.2. The age of Titan's surface

The relative age of planetary surfaces is often defined by the abundance of impact craters, as these form at a more-or-less uniform rate. With the notable exception of regions on Enceladus, the surfaces of the Saturnian satellites were revealed by Voyager imaging to be heavily cratered, and the pre-Cassini expectation (Lorenz, 1997) was therefore that Titan would be similar. It was noted that the present-day atmosphere is thick enough that (as at Venus) impactors smaller than about 1 km diameter would be slowed and/or disrupted, and thus craters smaller than 10–20 km diameter would be much less abundant (Artemieva and Lunine, 2003; Korycansky and Zahnle, 2005).

Cassini's first RADAR pass, TA in October 2004, revealed no obvious impact structures, whereas even that observed 0.5–1% of Titan's area would be expected to contain several craters if this pre-Cassini model were to hold. The subsequent pass T3 in February 2005 (Elachi et al., 2006), however, observed two – including what is still the largest crater (Menrva, 440 km diameter) and one of its best-preserved, Sinlap (80 km). Once mapping coverage had reached ~10% by T18, a survey (Lorenz et al., 2007) found the overall crater density is a factor of 5 higher than Earth, and has a size distribution slope very similar to Earth's indicating rapid obliteration of smaller structures by erosion and burial. Discrepant models of the 20–100 km impact crater production rate suggested an overall crater retention age of 100 Myr–1 Gyr. This assessment was confirmed and refined slightly, with a larger inventory of craters, by Neish and Lorenz (2012) who exposed – but could not resolve-the differing model assumptions that led to an interpreted age of 200–1000 Myr.

It had become clear at this point (with a few dozen craters – see also Wood et al., 2010) that the crater density is measurably non-uniform – craters being most abundant in the equatorial bright terrain Xanadu and its environs, and near-absent at high latitudes. This distribution has been interpreted as at least in part being due to hydrological effects – that low-lying 'wetlands' are less able to preserve crater topography (Neish and Lorenz, 2014).

Other surface features can place constraints on surface 'age'. The 150 m-high sand dunes at Titan's equator have a construction or reorientation timescale in the present wind regime of the order of 10s of thousands of years (giving them some 'memory' of previous phases of Croll-Milankovich astronomical climate cycles). The volume of material in the dunes (250,000 km^3 – Le Gall et al., 2011, or a global-equivalent thickness of several meters or a few times 1000 kg/m^2), if photochemically-derived, implies production timescales at present-day rates (3×10^{-13} $kg/m^2/s$) of ~10^{16} s or 300 Myr. Note that this number is derived from the observable dunes – if there is photochemically-derived material, whether sand-sized or not, that is not recognizable as dunes, then the photochemical production must have either proceeded for longer, or must have at some point been faster. As for other landforms, it is possible that the rates of fluvial erosion and/or deposition, including of evaporites, may be quantified, but at present understanding of the hydrological cycle – which appears to operate as long droughts punctuated by occasional rainstorms, and is strongly latitude-dependent - is not mature enough to allow useful surface age estimates.

The observed crater population (noting that there remain several tens of per cent of Titan's surface not observed by RADAR) is probably too sparse to be itself useful in defining regions of distinct ages, with the possible exception of Xanadu. An open question is whether the erosion and deposition processes clearly active on Titan (and responsible for the low number of craters overall) had perhaps buried Xanadu and then re-exposed it, accounting for the large number of degraded craters seen there. It would also be of interest if there are craters in the floors of Titan's seas.

More accurate topography data, and better information on the composition of the target material, would be useful in understanding crater formation and modification processes on Titan, since many aspects of the crater morphology (rather few are alike) are difficult to explain – only some first steps have been taken in that direction (Soderblom et al., 2010; Neish et al., 2015). An important question is the extent to which impact events may have excavated a possible water-ice crust (e.g. Le Mouélic et al., 2008; Janssen et al., 2016) from beneath the organic veneer that seems to cover most of Titan.

In summary, key open questions for the age of Titan's surface include:

- What is the reason for the difference in the crater population of Xanadu Regio from other regions on Titan?
- To what extent have internal activity, deposition, erosion and weathering caused the loss of an earlier surface?
- How have the rate and type of resurfacing processes changed over time?

3. Interior and surface

3.1. The location of the interior ocean

The Cassini/Huygens mission provided important insights on Titan's interior structure, such as the presence of a global water ocean at depth, making Titan one member of the Ocean Worlds family. However, major unsolved mysteries remain to understand its interior structure and the exchange processes between the interior and the atmosphere.

In addition to the hydrocarbon seas and lakes at its surface, Titan's interior contains a deep ocean which is, as on Europa, Ganymede, and Enceladus, likely composed of salty water. The first hint came from the analysis of the electric signal acquired during the descent of the Huygens probe in January 2005 (Beghin et al., 2012). The Huygens Atmospheric Structure and Permittivity, Wave and Altimetry (HASI–PWA) instrumentation observed electromagnetic waves. It was designed to enable the detection of Schumann resonances which are electromagnetic waves bouncing between two conductive layers. On Earth, these waves are triggered by lightning and bounce between the ionosphere and the oceans. On Titan, no lightning has been observed. On the other hand, similar waves can be generated by the variations of the ambient magnetic field during Titan's strongly eccentric orbit around Saturn (Beghin et al., 2012). The Extremely Low Frequency (ELF) wave observed at around 36 Hz displays all the characteristics of the second harmonic of a Schumann resonance. Using a simplified model for the Schumann resonance and the measurement of the atmospheric conductivity from the HASI-PWA instrument, Beghin et al. (2012) were able to derive the physical characteristics of the resonating cavity, including the depth of 65-km (±15-km) of the lower conductive surface. If this surface is interpreted as the boundary between the icy shell and a salty ocean,

Titan's outer shell would be about 65 km thick. However, a layer with a conductivity many orders of magnitude lower than that of a salty ocean could produce the same effect.

The presence of an ocean was demonstrated by the measurement of Titan's time variable gravity field inferred from a series of dedicated gravity flybys of Titan (Iess et al., 2012). Because of the large value of its orbital eccentricity of 0.029, Titan is subject to large variations of tidal forces during its 16-day orbit around Saturn. The moon responds to the external field with a time-variable response field measured by the k_2 Love number. Cassini's measurement ($k_2 = 0.589 \pm 0.150$ and $k_2 = 0.637 \pm 0.220$ under different assumptions; Iess et al., 2012) indicates (i) the presence of an ocean decoupling the icy shell from the interior (Iess et al., 2012) and (ii) the relatively high density of this ocean (Mitri et al., 2014) consistent with a high salinity. Unfortunately, the determination of k_2 does not provide any information on the depth of the ocean, and puts only weak constraints on the thickness of the shell.

Titan's interior is not as differentiated as its Jovian cousin Ganymede. Titan and Ganymede are very close in terms of radius and density. The Galileo mission demonstrated that Ganymede is fully differentiated with a liquid iron core where its intrinsic magnetic field is generated (Kivelson et al., 1996) and a deep ocean revealed by the induced magnetic field (Kivelson et al., 2002; Saur et al., 2015). Assuming hydrostatic equilibrium, the value of the moment of inertia, a measure of the degree of differentiation, is consistent with a fully differentiated moon with an inner liquid iron-rich core overlaid by a silicate mantle, a layer of high-pressure ices, a global ocean and an icy crust. For Titan, the value of degree 2 gravity coefficients (Iess et al., 2010) leads to a much larger value of the moment of inertia, suggesting that Titan's interior structure is made of a low density silicate core overlaid by the H_2O layer (Castillo-Rogez and Lunine, 2010). Whether the H_2O layer includes a high-pressure ice layer between the deep ocean and the silicate core depends on the thickness of the ice crust, a thicker ice crust meaning a thicker high-pressure ice layer (Fig. 2), and on the salinity of the ocean (Sotin and Kalousova, 2016) (Fig. 2). Whether the ocean is in contact with the silicates of the core has to be considered as an unsettled question because it depends on two quantities (thickness of the ice crust and salinity of the ocean) which are poorly constrained by the Cassini mission.

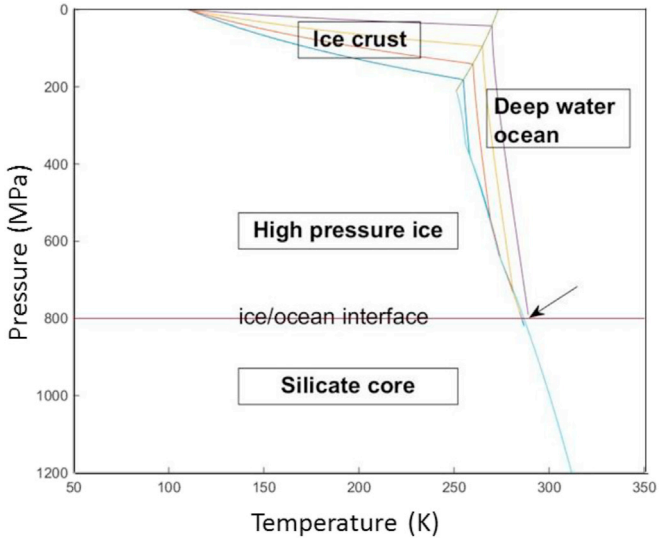

Fig. 2. Temperature profiles versus pressure for models that fit the value of the moment of inertia inferred from the degree 2 gravity coefficients obtained by the Cassini mission. If the crust is thin (purple curve), models predict that the ocean is in contact with the silicate core. If it is thick (light blue curve), a high-pressure ice layer is present between the ocean and the core (Sotin and Kalousova, 2016). (For interpretation of the references to color in this figure legend, the reader is referred to the Web version of this article.)

Finally, Titan's shape provides some hint on the structure of its icy crust. Nimmo and Bills (2010) determined that the long wavelength topography has an amplitude larger than that expected from tidal and rotational deformation. Their explanation is that the crustal thickness varies with latitude. The Airy model that they suggest provides best fit of the topography and gravity data for a crustal thickness of 100 km. It also rules out the possibility of convection in the icy crust. Alternatively, Choukroun and Sotin (2012) suggest a Pratt model (lateral density variations) where the density at the poles is larger due to the formation of dense ethane clathrates. Looking at higher degrees, Hemingway et al. (2013) report a negative correlation between the degree 3 gravity and topography. Their analysis implies that the rigid part of the ice crust is at least 40 km thick. However, a clear picture of the structure of the ice crust, with key information on its geological evolution, requires the determination of higher degrees in the expansion of the gravity and topography fields. Such measurements can only be acquired by an orbiter.

The presence of CH_4 (methane) and ^{40}Ar into Titan's atmosphere requires geologically recent exchange between the interior and the atmosphere. Methane is irreversibly transformed in the atmosphere and its presence implies a supply mechanism. Similarly, ^{40}Ar comes from the slow decay of ^{40}K (half-life of 1277 Myr) which is contained in the silicate fraction, suggesting processes to transfer ^{40}Ar from the silicate fraction to the atmosphere. Unfortunately, the Cassini/Huygens mission has not provided clues on the extent and timing of these processes. Future missions able to measure noble gases and their isotope ratios would provide such information. No active volcanism has been detected (see Section 3.2).

Important open questions include:

- How thick is the ice shell, and how deep is the global ocean? Is it in contact with a silicate core at the lower boundary, or a high pressure ice layer?
- Have exchanges occurred between the surface and the interior? This would provide a pathway for the transfer of the complex organic material produced in the atmosphere and falling onto the surface to the deep water ocean.
- Is the silicate core in contact with the deep water ocean? This would provide an interface similar to the terrestrial sea-floor, one of the places where life may have emerged on Earth.

3.2. Cryovolcanism on Titan

The existence of features formed by cryovolcanic activity has been the subject of some controversy, which is unlikely to be resolved by Cassini data, mainly due to imagery and spatial coverage limitations. Our interpretations of cryovolcanic features on Titan rely on data from Cassini RADAR (including SAR - Synthetic Aperture RADAR, stereogrammetry, SARTopo, and radiometry) and data from the Visible and Infrared Mapping Spectrometer (VIMS). Interpretations are based on morphology and, in some cases, differences in composition from surrounding terrains as shown by VIMS (Solomonidou et al., 2018), as well as temporal variations. To date, cryovolcanoes on Titan have not been caught red-handed, i.e., no hot spot has been detected. However, the detection of thermal activity at Titan's surface using radiometry data (which is sensitive to variations of ~1 K) or VIMS would require Cassini's instruments to be observing the right locations at the right times. Given the consensus that cryovolcanism is not ubiquitous on Titan (Lopes et al., 2010), this is unlikely to happen.

The possibility of finding cryovolcanic features on Titan had been discussed prior to Cassini (e.g. Lorenz, 1993, 1996), including the prediction that the presence of a thick atmosphere on Titan would suppress the vesiculation of bubbles in a cryomagma, reducing the distribution of explosive products, and will speed the cooling of cryolavas (Lorenz, 1993). Results suggesting cryovolcanism came early on the mission. The GCMS instrument detected the radiogenic isotope of argon 40 in Titan's

atmosphere (Niemann et al., 2005), suggesting that the atmosphere was at least partly generated by outgassing from the interior. Sotin et al. (2005) proposed that a feature, Tortola Facula, observed from Cassini's VIMS might be cryovolcanic in origin, and suggested that the upwelling of large cryovolcanic plumes may be releasing sufficient methane into the atmosphere to account for the known atmospheric composition. RADAR SAR images obtained later in the mission did not show evidence of cryovolcanic morphology for Tortola Facula but rather that the feature was a local topographic high similar to others elsewhere on Titan (Lopes et al., 2013).

The first Titan flyby using RADAR showed several features interpreted as cryovolcanic (Lopes et al., 2007), including a large (180 km diameter) volcanic construct named Ganesa Macula, possibly a dome or shield, plus several extensive flows, and three calderas which appeared to be the source of flows. However, additional data acquired by RADAR at a later time showed that Ganesa was an eroded feature rather than a dome or shield. Alternate, exogenic interpretations for Ganesa and other putative volcanic features have been suggested (Moore and Howard, 2010; Moore and Pappalardo, 2011). Other evidence for cryovolcanism was put forward by Nelson et al. (2009a,b) using temporal variations seen in VIMS data that suggested that active cryovolcanism, or at least degassing, was taking place from two areas, Hotei Regio and east Xanadu, which also showed evidence of cryoflows (e.g., Wall et al., 2009). However, other analyses of VIMS data (Soderblom et al., 2009; Solomonidou et al., 2016) disagreed with this interpretation. Soderblom et al. (2009) concluded that the VIMS observations up to that time did not provide any compelling evidence for temporal variations on Hotei Regio, attributing the Nelson et al. (2009a,b) result to the observational limitation of the dataset and not to actual surface changes. Solomonidou et al. (2016) revisited the same dataset and included additional observations up to 2009, using a radiative transfer code to correct for atmospheric effects, and reported that the area remained unchanged compared to surrounding areas for that period of time (2005–2009).

The strongest evidence for cryovolcanic features on Titan was put forward by Lopes et al. (2013) who combined topography, SAR imaging and VIMS data for a region that includes Sotra Patera, Mohini Fluctus, and Doom and Erebor Montes. Doom and Erebor Montes are tall mountains (Doom being >1 km high, Fig. 3a), Sotra Patera is a deep (>1 km) non-circular depression interpreted to be a collapse feature adjacent to Doom Mons (Fig. 3b). A lobate flow feature (Mohini Fluctus) appears to emerge from Doom Mons, other non-circular, collapsed depressions are located between the two Montes, and a series of flows surrounds Erebor Mons. Of particular interest is the fact that the area is totally devoid of fluvial channels, making a fluvial origin for the flows unlikely. Moreover, the dune field that lies between Doom and Erebor Montes indicates that this is a dry region. The fact that the depressions, including Sotra Patera, are not circular makes an impact origin unlikely for these features, furthermore, there is no evidence of any impact ejecta blanket surrounding the depressions. The occurrence of Titan's deepest known depression and several lesser depressions in such close proximity to some of the most substantial mountains on Titan make it unlikely that impacts—so rare elsewhere on Titan— could explain these features. VIMS data shows that the composition of these features is different from that of plains or dunes (Solomonidou et al., 2018). VIMS data analysis with the use of a radiative transfer code also indicated temporal changes for the area of Sotra Patera, which became brighter up to a factor of 2 in terms of pure surface albedo and brightness during one year (2005–2006), while other areas such as the area surrounding Sotra, and the undifferentiated plains and dunes, did not present any significant change for the same period of time (Solomonidou et al., 2016), suggesting a local phenomenon. The surface albedo variations, together with the presence of volcanic-like morphological features, suggest that the active regions are possibly related to the deep interior via cryovolcanic processes. New interior structure models of Titan and corresponding calculations of the spatial pattern of maximum tidal stresses (Sohl et al., 2014) also indicate that the Sotra complex is a likely region for activity.

The Sotra complex remains the strongest evidence that cryovolcanism happened on Titan. Cryovolcanism on Titan can explain outgassing over time to sustain the methane in the atmosphere (Sotin et al., 2005; Tobie et al., 2006) and has important implications for the satellite's astrobiological potential. Cryovolcanic features have been identified elsewhere in the solar system, including recently on Ceres (e.g. Krohn et al., 2016; Ruesch et al., 2016) and Pluto (e.g. Moore et al., 2016), suggesting that cryovolcanism is an important process for shaping the surfaces of icy bodies.

Principal questions concerning internal activity are:

- Is Titan currently, or has it been in the past, cryovolcanically active?
- Has Titan post-formation experienced large scale plate tectonics or crustal upheaval?
- How has internal activity affected the surface age in various different terrains?
- Has activity allowed mixing of ammonia/water ices with organic deposits from the atmosphere?

3.3. What is covering the surface?

Solving the controversy over whether or not water ice is exposed on Titan's surface depends on understanding Titan's atmospheric transmission and effects from scattering. Early analyses, e.g. Griffith et al. (2003) and references therein used the decreasing apparent reflectance in the 1–3 μm region of Titan's spectrum as evidence for water ice. Clark

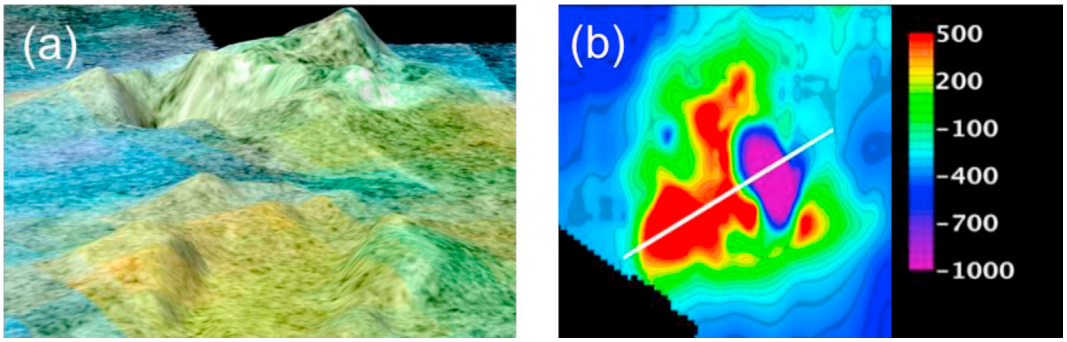

Fig. 3. (a) Cassini RADAR data and visible and infrared spectrometry were combined in this view of the Sotra Patera complex with colors showing compositional differences. Doom Mons, over 1 km high, is adjacent to the deepest depression so far found on Titan, Sotra Patera, an elongated, pit over 1 km deep. Green and yellow shows areas that appear cryovolcanic in origin. (Courtesy of R. Kirk, USGS). (b) Topographic profile of Sotra Patera showing pit is > 1 km deep, adjacent to Doom Mons, a mountain > 1 km high. The Sotra patera pit is not circular and unlikely to have been formed by impact. The length of the white trace is 100 km. Mohini Fluctus, a possible outflow, extends to the northeast (upper right). (For interpretation of the references to color in this figure legend, the reader is referred to the Web version of this article.)

et al. (2010) used the 2.7 and 2.8-μm spectral windows (where methane gas opacity is low) as an indicator to show incompatibility with water ice, as water ice is significantly more absorbing at 2.8-μm compared to 2.7-μm. Early radiative transfer models in the Clark et al. (2010) study did not have atmospheric absorption coefficients that were measured for the conditions on Titan, prompting debates over the true 2.7/2.8 μm ratio. Barnes et al. (2013a) derived the transmission spectrum of Titan's atmosphere using specular reflections from methane lakes, showing that the derived spectrum was very reddened. Hayne et al. (2014) computed optical depths using VIMS solar occultation data that probed deeper into Titan's atmosphere than Clark et al. (2010). The optical depths resulting were: 2.7 μm: 0.8 ± 0.2 and 2.8 μm: 0.22 ± 0.02 and this wavelength difference in optical depths must be regarded in the spectra as a function of incidence or emission angle with differing optical path lengths.

These optical depths would predict 2.8/2.7-μm reflectance ratios of 1.8 at 60° incidence angle and more than 3 at 75° incidence angle. However, the ratio remains unchanged with observed incidence angles as shown in Fig. 4, thus the Hayne et al. model for predicting the ratio is incomplete. The transmission measured in a solar occultation and in a specular reflection measurement is reddened by scattering in the atmosphere. The Barnes et al., and Hayne et al., studies did not account for the reddening. Measurements of a diffuse surface are not reddened in the same way by scattering, thus no such reddening is observed in reflectance measurements of Titan's extended surface. Rodriguez et al. (2016) presented new atmospheric radiative transfer models for Titan with new line parameters for Titan atmospheric conditions. These new models closely model the 2.7 and 2.8 μm windows in agreement with the observed VIMS data for Titan.

The incidence-phase dependence shown in Fig. 4, as well as the new radiative transfer models by Rodriguez et al. (2016) indicates little change in the 2.7/2.8 μm reflectance ratio by the atmosphere. This means that the high 2.8-μm reflectance rejects significant amounts of water ice from being exposed at the surface. Early studies of Titan's atmosphere only considered water ice as the cause of the 1–3 μm decrease in reflectance, partly due to lack of reference spectra of other likely Titan compounds. Clark et al. (2010) showed many organic compounds also display the decreasing reflectance characteristics. Kokaly et al. (2017a, b) published a new spectral library of compounds and many organics and ammonium compounds show decreasing reflectance characteristic compatible with Titan's spectrum, including the 2.7/2.8-μm reflectance ratio.

Some recent studies continue to use the short wavelength slope to

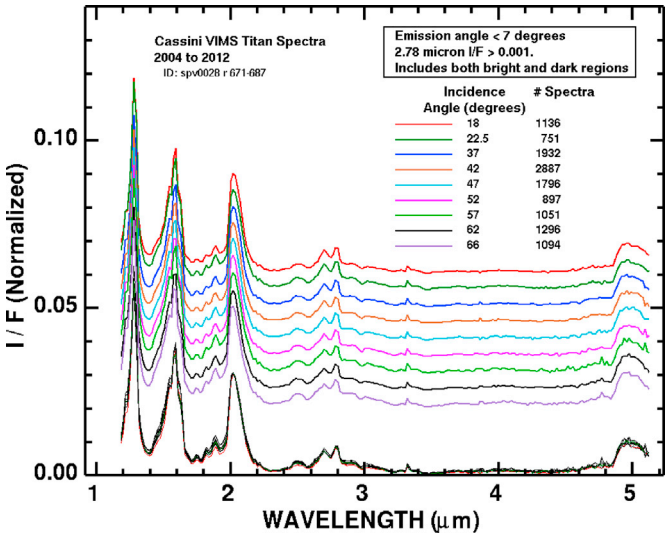

Fig. 4. average VIMS spectra of Titan measured at different incidence angles. There is effectively no change in the relative strengths in the different windows, including the 2.7 and 2.8 μm windows.

"identify" water ice in VIMS spectra. For example, Griffith et al. (2017) performed a Principle Components Analysis using wavelengths in four of Titan's spectral windows: 1.1, 1.3, 1.6, and 2.0 μm but not the much higher ice-sensitive 2.8 μm window. Regions shown by Griffith et al. to be high in water ice content show a high 2.8 μm reflectance relative to 2.7 μm, indicating water ice cannot be present at any significant level. Many organic and N-H bearing compounds decrease in reflectance from 1 to 2 μm like water ice (e.g. Clark et al., 2009, 2010, Kokaly et al., 2017a, b) and newer studies must account for all these facts. If that is done, many compounds can be rejected from being exposed on Titan's surface, including water ice, ammonia ice, carbon dioxide ice, and others.

In summary, new radiative transfer models and emission phase function data for Titan show that the reflectance properties of Titan's surface are incompatible with significant amounts of exposed water ice. New reflectance spectra of organic and ammonium compounds show compatibility with Titan's surface over the entire VIMS spectral range. However, identifications of specific compounds remains elusive except in a few isolated cases, like the benzene identified by Clark et al. (2010) or the ethane identified by Brown et al. (2008) where diagnostic absorptions were seen through Titan's atmospheric windows. The major remaining question is what are the actual compounds on the surface, and that cannot be answered until improved radiative transfer models are completed.

Key questions:

- What simple and complex compounds are covering Titan's surface, and how do these vary from region to region?
- How does the surface change on short and long timescales, e.g. rain storms, aerosol deposition?

In the near future, some of the compositional ambiguities may be resolved by the higher spectral resolution in the near-IR that will be achievable using the NIRSpec instrument on the James Webb Space Telescope (JWST), as described in Nixon et al. (2016).

3.4. Lakes and seas – distribution

Hydrocarbon lakes and seas occupy 1.1% of Titan's global surface area (Hayes et al., 2011) and have a total volume of ~70,000 km^3 (Hayes, 2016; Lorenz et al., 2008). They are restricted to polar latitudes (55°–90°) and occupy 40 times more surface area in the north compared to the south (Hayes et al., 2011). This dichotomy has been attributed to Saturn's current orbital configuration, where southern summer solstice nearly aligns with perihelion. As a result, Titan's south polar terrain receives 25% higher peak flux during summer than the north (Aharonson et al., 2009). This configuration is transient, as apsidal precession changes the position of Saturn's seasons relative to its eccentric orbit on timescales of tens to hundreds of thousands of years. In the south polar terrain, dry broad depressions (see Fig. 5 A) have been suggested to represent paleoseas that were filled during an earlier epoch (Hayes et al., 2011). However a lack of 5-μm bright material, interpreted in the north as evaporite, confounds this interpretation in the absence of an efficient removal or burial mechanism (MacKenzie et al., 2014). Observations of 5-μm bright material near Titan's equator and mid-latitudes may also represent evidence of past standing liquid at these locations (MacKenzie et al., 2014; Vixie et al., 2015). Morphologic and compositional evidence acquired from higher resolution data than Cassini could provide will be necessary to test these hypotheses and determine the distribution of surface liquid in Titan's past.

Titan's lakes are found within a common morphologic unit and its seas, or Mare, appear to share a common geopotential surface (Hayes et al., 2017). Basin floor elevations amongst features interpreted as dry lakebeds suggest local control by a phreatic surface (Hayes, 2016), but the degree of connectivity amongst the lakes and seas remains an open question. Similarly, sediment transport pathways within Titan's polar terrain remain obscure. Regardless, secondary erosional and depositional

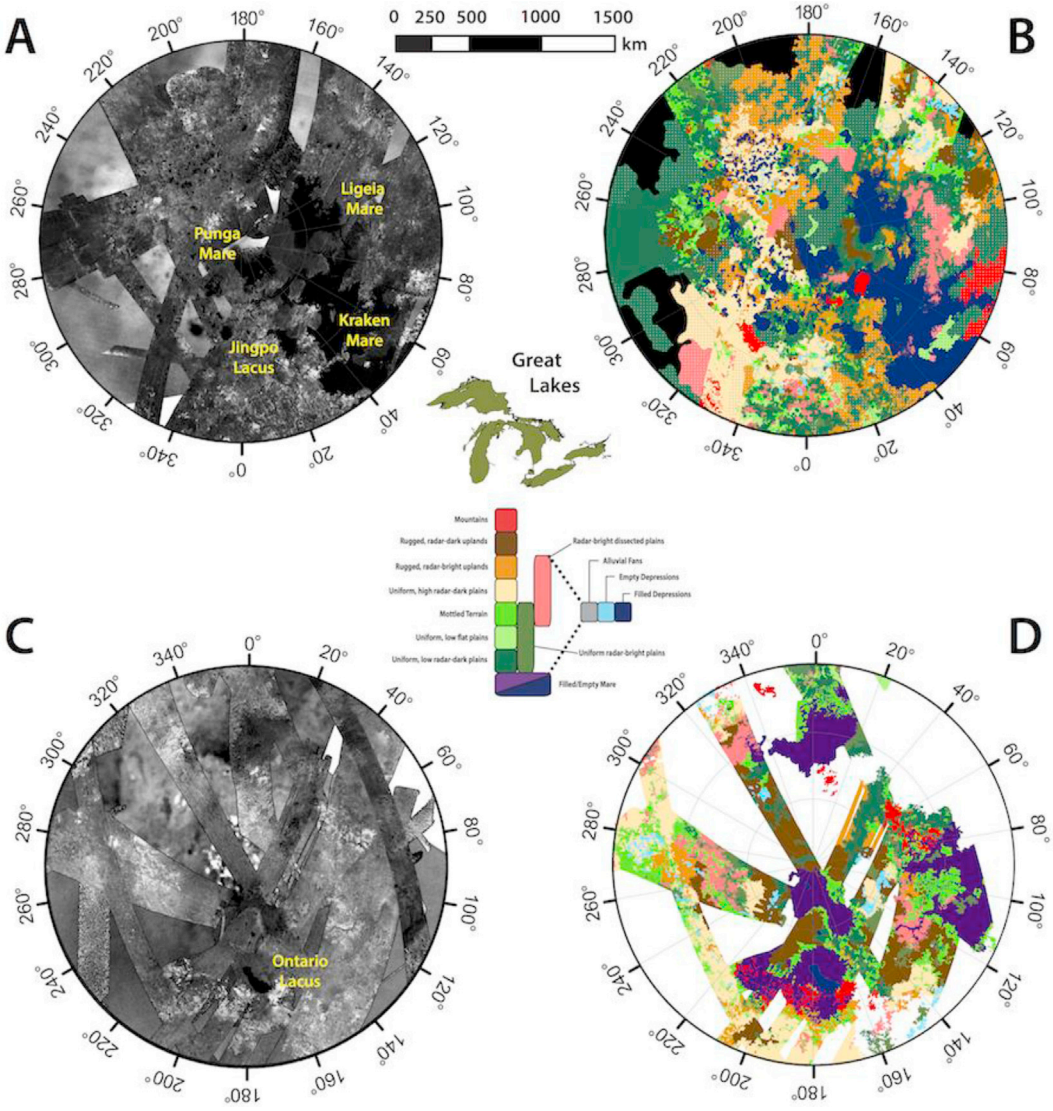

Fig. 5. Polar distribution of hydrologic features on Titan derived from Cassini data acquired through January 2015 (flyby T108). All four panels are stereographic polar projections centered at 90°N (A/B) and 90°S (C/D) and extend to 55°N (A/B) and 55°S (C/D), respectively. The panels on the left depict false-color Synthetic Aperture Radar (SAR) mosaics (gold) overlying near-infrared Imaging Science Subsystem (ISS) maps (gray), with Titan's Maria and larger lakes identified. The panels on the right show the morphologic mapping units identified by Birch et al. (2017). The relative topography of the mapped units is represented by the vertical arrangement of boxes in the central legend. Underlying terrain is mapped in red, the sedimentary undulating plains in orange, and the dissected uplands in various shades of green. Filled lakes and seas are shown in blue, whereas potential paleoseas and empty lake basins are shown in purple and cyan, respectively. An outline of Earth's Great Lakes in North America is included for scale. Adapted from Fig. 1 in (Hayes, 2016). (For interpretation of the references to color in this figure legend, the reader is referred to the Web version of this article.)

landforms, including alluvial fans (Birch et al., 2016), deltas (Wall et al., 2010), and large river valleys that feed into the Mare (Burr et al., 2013), are found at both the north and south and hint at a complex source-to-sink sediment transport system. Titan's polar terrain is geologically distinct from the rest of body, and understanding its evolution remains an essential question that will require a future mission to unravel.

As compared to Earth, where the size-frequency distribution of lakes and ponds follow a power law relationship, Mars and Titan exhibit a dearth of small lakes relative to their cumulative totals (Hayes, 2016). On Mars, this discrepancy has been attributed to differential erosion destroying smaller features over the past 3.5 Gyr (Cabrol and Grin, 2010). On Titan, an active hydrologic system suggests that differential erosion is unlikely to explain departure from a power law size-frequency distribution. An alternative explanation is that there is a scale dependence to basin formation (Hayes, 2016). While Titan's larger lakes and Mare appear to be formed through inundation of preexisting well-drained landscapes (Hayes et al., 2008; Stofan et al., 2007), the formation mechanisms for the smaller lakes, known as sharp edged depressions (SEDs), remains unknown (Hayes et al., 2017). While the lack of inflow and outflow channels at the resolution of Cassini images and plan-view morphology have been used to argue for karst-like processes (e.g., Mitchell et al., 2008), hundred-meter-scale raised rims found on many of Titan's SED (Michaelides et al., 2016; Hayes et al., 2017) are inconsistent with traditional karst terrain (Ford and Williams, 1989a,b). The significant depth (>600 m) of several of these features presents a mass conservation problem as it is unclear where the eroded or dissolved material has gone (Hayes et al., 2008). Similarly, it is unclear how Titan's organic budget can support >600 m of volatile organic layers in sections of the polar terrain. Water ice is insoluble in liquid hydrocarbon and cannot support dissolution or sublimation-based processes (Perron et al., 2006). Understanding the formation of Titan's SEDs is intimately linked

to a general understanding of Titan's volatile cycles and remains a major outstanding question post-Cassini.

While Cassini has unveiled the distribution, morphology, and relative elevation of Titan's lakes seas, several open questions remain for future exploration.

- Were the potential paleobasins that have been identified in the south polar terrain truly once liquid filled?
- How are lacustrine basins, particularly the sharp edged depressions, formed?
- While available topography suggests at least local subsurface communication, the extent that the lakes are globally or regionally connected remains unknown.
- Similarly, the transport pathways for material removed during lacustrine basin generation and expansion remains a mystery.
- And finally, where there ever lakes and/or seas in the mid-latitudes or equator?

Many of these questions can be addressed by higher-resolution images acquired by a future in-situ or orbiting spacecraft (e.g. Leary et al., 2007; Coustenis et al., 2009; Mitri et al., 2018).

3.5. Lakes and seas - composition

For the majority of the Cassini mission the depth and composition of Titan's liquid bodies remained elusive. While liquid ethane was positively identified in Ontario Lacus by Brown et al. (2008), the 2007 VIMS data used in the study was only sensitive to ethane's presence, not its abundance. Similarly, the identification of 5 μm bright deposits interpreted as evaporate, also at Ontario Lacus, by Barnes et al. (2011) hinted at more complex liquid compositions but could not identify the constituents. While several studies (e.g., Elachi et al., 2004; Lorenz et al., 2008; Lunine and Lorenz, 2009; Brown et al., 2008; Hayes et al., 2010; Cordier et al., 2012; Cornet et al., 2012) used indirect measurements to estimate the depth of Titan's lakes and seas, the first direct measurements of lake depth did not occur until the end of the Cassini Solstice Mission.

In May 2014, a subsurface reflection was detected from the seabed of Ligeia Mare during a closest-approach altimetry flyby (Fig. 6). This

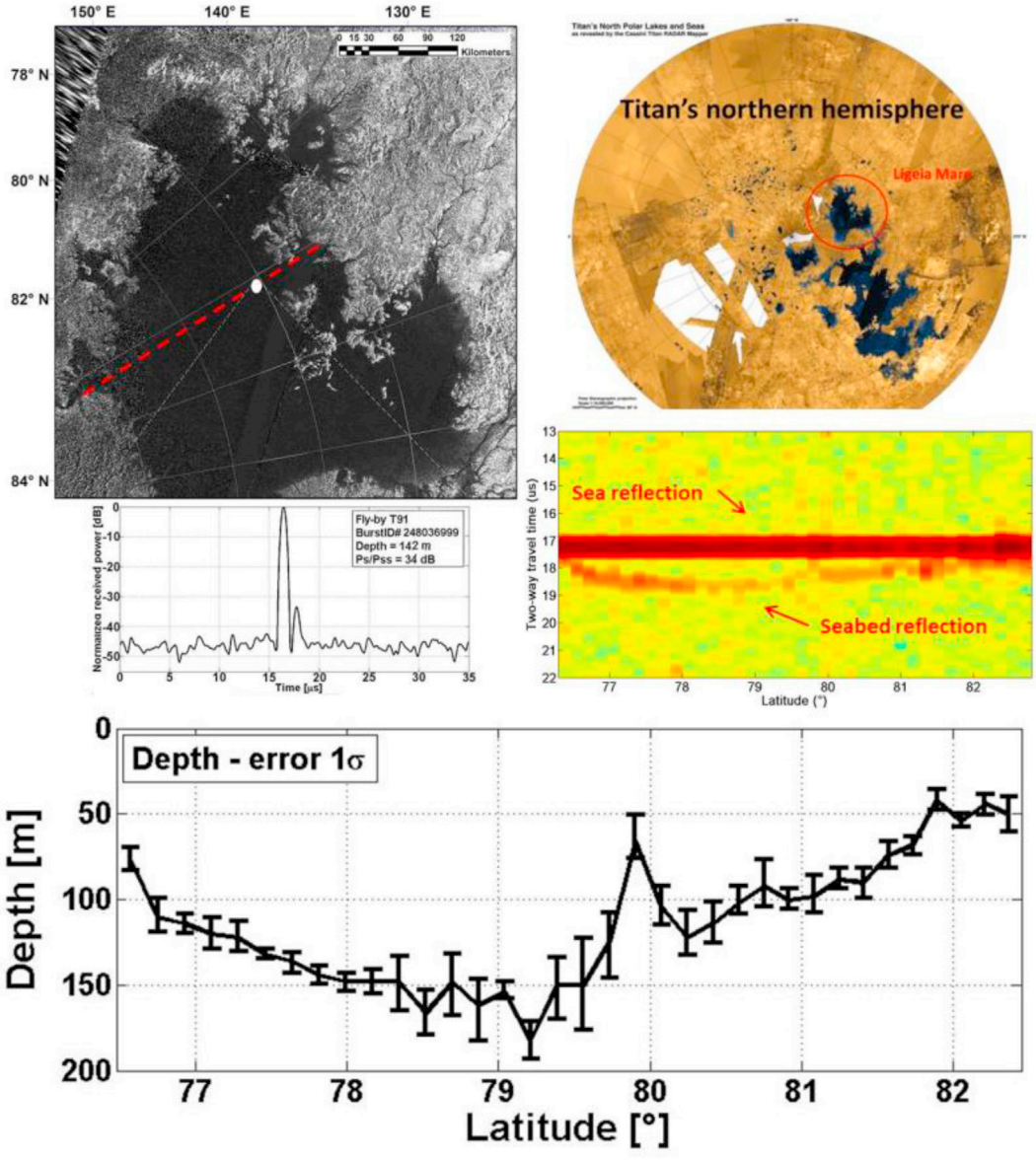

Fig. 6. Ligeia Mare, Titan's second largest sea (top). Echo response over the sea (middle left). Seabed topography of Ligeia (middle right). Bathymetry of Ligeia (bottom). (adapted from Mastrogiuseppe et al., 2016).

observation revealed a new and exciting capability of the Cassini RADAR during the T91 closest-approach altimetry flyby and jump started a campaign to measure the depth and composition of Titan's largest liquid bodies, creating the first extra-terrestrial bathymetric profiles. Ligeia was determined to have a depth of 170 m at the deepest point along the observed track (Mastrogiuseppe et al., 2014). The observed bathymetric tracks, combined with SAR imagery, were then used to determine the total volume of the basin, which was found to contain ~10,000 km^3 of liquid hydrocarbons. The analysis of the RADAR signal received from the seafloor was also used to estimate the liquid attenuation at Ku band and constrain the loss tangent of the sea to be $4.4 \pm 1 \times 10^{-5}$ (Mastrogiuseppe et al., 2016). Assuming a methane-ethane-nitrogen composition, using the laboratory measurements of Mitchell et al. (2015) and applying the Lorentz-Lorenz formulation, the measured loss tangent of Ligeia Mare was equivalent to a mixture of approximately 71% CH_4: 12% C_2H_6: 17% N_2, indicating that Ligeia is methane dominated. If trace amounts of higher-order hydrocarbons are present as well (e.g., propane is expected at the ~1% level), the fraction of methane will increase. This result demonstrated that Titan's seas are incredibly transparent and are methane-dominated. This result is surprising given the large quantities of liquid ethane that should have been produced by photolysis of methane in the upper atmosphere. If the ethane is not concentrated in the lakes and seas, it must be sequestered in another reservoir (e.g., subsurface liquid deposits or sequestration in crustal clathrate hydrate). Regardless, methane-dominated compositions are consistent with equilibrium models of Titan's sea composition predicted by Glein and Shock (2013) and Tan et al. (2015).

Following the T91 observation of Ligeia Mare, observations of Kraken Mare and Punga Mare were planned and executed in August 2014 (T104) and January 2015 (T108), respectively. While most of the seafloor was not detected at Kraken, suggesting the sea was either too deep or too absorptive in these areas to observe any return from the seafloor, shallow areas near Moray Sinus did return subsurface detections. At Punga Mare, a clear detection of the subsurface was observed with a maximum depth of 120 m along the interrogated track of the sea floor. The subsurface signals received during these fly-bys indicate that Punga has a similar loss-tangent to Ligeia.

Applying the same techniques used for the detection of the seafloors of Ligeia Mare and Punga, Mastrogiuseppe and colleagues reprocessed the T49 data acquired over Ontario Lacus on 21 December 2008. The optimized signal processing adopted super resolution techniques and dedicated taper functions to reveal the presence of lakebed signal reflections. The team used RADAR altimetry simulator to retrieve information from the saturated bursts and determine the liquid depth and loss tangent of Ontario Lacus (Mastrogiuseppe et al. 2018).

Assuming a similar ternary composition, the loss tangent at Ontario Lacus ($7 \pm 3 \times 10^{-5}$) is consistent with ~47% CH_4, ~40% C_2H_6, and ~13% N_2. As with Ligeia, however, the methane abundance would need to increase if higher-order hydrocarbons are present in order to keep the loss tangent at observed levels. Regardless of whether ethane or larger molecules are the cause, Ontario Lacus has a greater loss tangent and appears to contain more high-order hydrocarbons than Ligeia Mare. The higher loss tangent could result from an increased abundance of more involatile hydrocarbons and/or nitriles or suspended particulates. These particulates could also explain the differences observed between the loss tangent derived from altimetry ($\sim 7 \times 10^{-5}$) and the order of magnitude higher loss tangent ($\sim 6 \times 10^{-4}$) derived by Hayes et al. (2010) using a combination of near-shore (within a few km of the shoreline) SAR backscatter and near-shore altimetric slopes. If solutes or suspended particles were concentrated in the near-shore regions of Ontario Lacus, their presence could result in an increase in the near-shore microwave absorptivity. This scenario would be consistent with the observation that the near-shore ethane bands, unlike central Ontario Lacus, are not saturated in VIMS observations (Brown et al., 2008).

Measuring the bathymetry and microwave absorptivity of Titan's seas was not planned and represents an exciting addition to the discoveries made by the Cassini spacecraft. As with many of Cassini's discoveries, however, the answer to one question has presented a collection of new questions:

- If the lakes and seas are methane-dominated, where is all of the ethane produced by photochemistry in Titan's atmosphere (see §2.1)?
- What is the variability of composition amongst the lakes and seas?
- Similarly, what are the abundances of higher-order hydrocarbons in Titan's lakes and seas?
- What is the greatest depth of Kraken Mare, Titan's largest sea?
- Why is Ontario Lacus compositionally distinct from the northern seas?

Answering these questions will require in-situ exploration (e.g. Lorenz and Mann, 2015) able to provide sea and sea floor chemistry. Today the detailed composition of Titan's lakes and seas remains still unknown.

3.6. *What complex, possibly prebiotic chemistry is occurring on Titan's surface?*

The Voyager flybys of Titan in 1981 led to the determination of the main composition of its atmosphere and the detection of many organic compounds. Since then, the largest satellite of Saturn has become a key astrobiological object, a natural chemical laboratory at the planetary scale to study possible prebiotic chemistry (Raulin et al., 2012). In the 1980s it was believed that Titan's surface was covered by a global ocean of liquid methane and ethane (Sagan and Dermott, 1982; Lunine et al., 1983; Lunine and Stevenson, 1985; Lunine and Rizk, 1989; Dubouloz et al., 1989). Physical-chemical processes of interest for astrobiology were assumed to occur in the different phases of Titan's 'geofluid': the gaseous atmosphere, the aerosols and the liquid surface, with many exchanges and couplings between these phases. Within this context, the aerosols, thought to be mainly organic, were presumed to play a key role, concentrating the organics in the atmosphere and bringing them to the surface. However, with a liquid ocean made of hydrocarbons, the chemical evolution following the sedimentation of aerosols seemed very limited. Moreover, the corresponding chemistry involved almost exclusively C, H and N atoms, excluding the potential occurrence of biochemistry as we know it that requires oxygen. Nevertheless, some possibilities of a biochemistry based on 'amono' analogs, where oxygen atoms are replaced by NH groups, has been considered (Raulin and Owen, 2002). This was speculation however, as much as the organic composition of the aerosols themselves. Their composition was assumed to be similar to that of 'tholins' (Sagan and Khare, 1979; Khare et al., 1986 and references therein) - laboratory analogs to organic atmospheric haze produced by experimentally simulating the chemical evolution of Titan's atmosphere. These exhibited interesting properties for astrobiology, releasing amino acids when hydrolyzed by very acidic aqueous solutions (Khare et al., 1986). Many studies were subsequently carried out on these tholins (see review by Cable et al., 2012), showing highly variable properties depending on the experimental conditions used to produce them (Coll et al., 2013).

By the mid 1980s, it was suggested that there was no global ocean on Titan (Owen, 1985). This was confirmed in the late 1990s, when it was possible to observe Titan's surface first from the Hubble Space Telescope (HST: Smith et al., 1996) and then from ground-based observatories with adaptive optics. But this was clearly demonstrated as soon as Cassini-Huygens entered the Saturn system and started to observe Titan. The observations of Titan by the VIMS, Imaging Science Subsystem (ISS) and RADAR instruments on the Cassini orbiter and, in January 2005, the Descent Imager and Spectral Radiometer (DISR) on the Huygens probe, showed that its surface is very diversified, with dunes, fluvial networks, craters, potential cryovolcanoes and lakes/seas. Thus one should now consider these different geological features to look for any possible evolution of the aerosols after they sediment on Titan's surface (Fig. 7). Another result from Cassini-Huygens of importance for astrobiology is

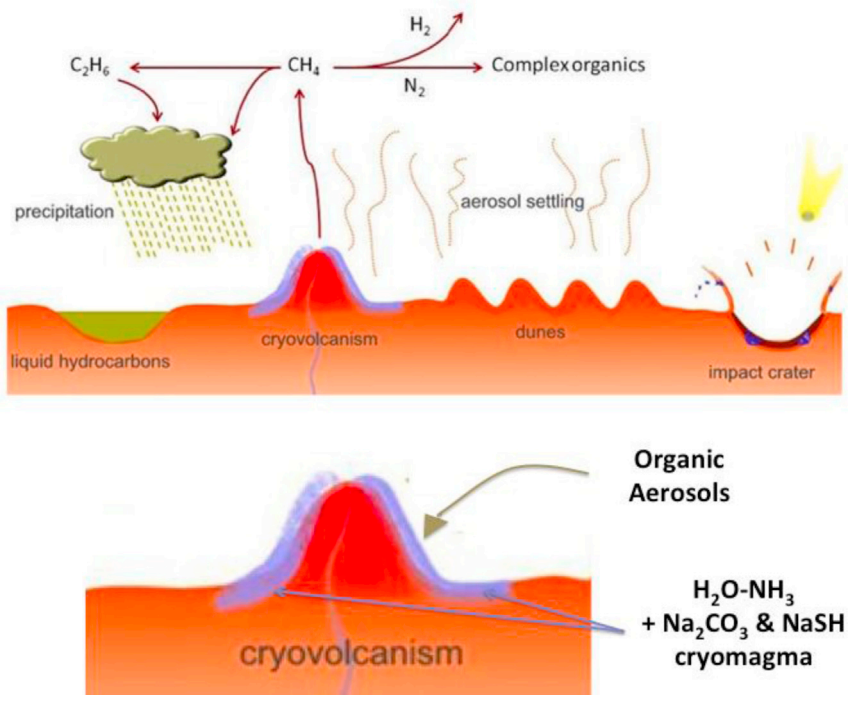

Fig. 7. The different geological features on Titan's surface in interaction with the atmospheric aerosols (top) with a zoom on the particular case of the cryovolcanic areas (bottom). (adapted from Poch et al., 2012).

the chemical analysis of the aerosols by Huygens instruments. The sampling and pyrolysis of the collected particles by the Aerosol Collector-Pyrolyzer (ACP), followed by molecular analysis by the GCMS showed that the aerosols are made of a refractory nucleus composed of C, H and N-atoms, covered by volatile condensed compounds (Israel et al., 2005, 2006). This behavior is similar to that of some tholins (see Cable et al., 2012 for review), in particular those synthesized from N_2/CH_4 gas mixtures using a cold plasma device (Coll et al., 2013). This justified the use of such tholins as analogs for Titan's aerosols, although there is now evidence that in detail the spectral properties of many laboratory analogs do not match the Titan observations (Hörst, 2017).

Among the locations of importance for astrobiology on Titan, the (still hypothetical) cryovolcanic areas are particularly interesting. Indeed, it can be supposed that the cryolava, whose composition is assumed to be close to that of the internal water-ammonia ocean, may chemically interact with the deposited aerosols, producing organics including O-compounds of biological interest (Fig. 7). Since the arrival of the Cassini mission in the Saturn system, several experimental studies have been carried out to simulate such a possible chemical evolution using Titan tholins and water-ammonia solutions. (Neish et al., 2009, 2010; Ramirez et al., 2010; Poch et al., 2012). More recently, similar work was done with 'Titan' tholins produced and collected in clean laboratory conditions, without oxygen contamination (Brassé et al., 2016). The tholins were mixed with different aqueous solutions representative of the hypothetical cryolava assumed to be similar to that of the internal ocean. The composition of the subsurface ocean – hypothesized to include 5 wt % ammonia - was determined by acido-alkaline calculations (Brassé et al., 2016). The most abundant minor species are carbonate and hydrogen sulfide ions. The hydrolysis of oxygen-free tholins, in the presence or absence of carbonates, leads to the formation of several compounds of astrobiological interest, in particular amino acids. The most abundant product in all these experiments is urea. The impact of carbonates is very important in the chemical processes (Brassé et al., 2016). Similar studies must now be completed with hydrogen sulfide ions.

Finally, it is worth noting that impact craters are among the most important targets for future missions to explore, since the (aqueous) impact melt allows the chemical introduction of oxygen via hydrolysis into Titan's abundant photochemical organics, permitting the synthesis of pyrimidines, amino acids and other prebiotic compounds of particular astrobiological interest (e.g. Artemieva and Lunine, 2005; Neish et al., 2010). In this respect, it should be noted that crater melt and vapor can reach higher temperatures than surface-exposed cryovolcanic material is likely to attain, and thus reactions can proceed faster such that impact melt sheets may permit more advanced aqueous synthesis.

Important issues surrounding Titan's prebiotic chemistry include:

- Are there sulfur-containing compounds and/or ammonia exposed on the surface that could indicate active cryovolcanism?
- Are there amino acids or other compounds of biological interest in the surface formed by interaction of atmospheric products with surface melts?

For future discrimination on Titan, several of the products obtained in laboratory simulations have strong spectral signatures in the infrared, particularly in the 5–20 μm region. Infrared spectra of solid phase glycine and alanine exhibit strong features around 7 μm, and urea around 10 μm. They could be searched for in the IR-spectra of the potentially cryovolcanic areas of Titan. Future IR observations of Titan with a large spectral range and a spatial resolution of less than 100 m, high enough to zoom on potential cryovolcanic areas may be able to detect these compounds of astrobiological interest - especially the most abundant product, urea - on the surface of Titan. This could be achieved from a near-surface platform like the one proposed with the TandEM mission (Coustenis et al., 2009). A detection could be very efficiently achieved with a mission allowing surface sampling and in situ molecular analysis with high resolution mass spectrometry, such as Orbitrap (Briois et al., 2016), and gas chromatography techniques. The identification of amino acids and salts on Titan's surface could be a biomarker of complex prebiotic-like chemistry.

4. Lower and middle atmosphere

4.1. Hydrogen profile mystery

The third most abundant species in Titan's atmosphere is molecular

hydrogen with a tropospheric/lower stratospheric mole fraction of 0.001 derived from Voyager and Cassini infrared measurements (Courtin et al., 1995, 2008; Samuelson et al., 1997) and by direct measurement of Huygens GCMS (0.001 at 100 km, Niemann et al., 2010). The globally averaged thermospheric H_2 mole fraction profile from the Cassini Ion Neutral Mass Spectrometer (INMS) measurements (e. g., mole fraction = 0.004 at 1175 km, Waite et al., 2005; Cui et al., 2008) implies a small positive gradient in the H_2 mixing ratio from the tropopause region to the lower thermosphere (~950–1000 km), which drives a downward H_2 integrated flux into Titan's troposphere comparable to the H_2 escape rate out of the atmosphere ($\sim 1 \times 10^{28}$ H_2 s^{-1}, Strobel, 2010, 2012).

Further analysis of Cassini Composite Infrared Spectrometer (CIRS) measurements by Courtin et al. (2012) yielded a latitudinal variation in the tropospheric mole fraction. They found that the winter northern polar value increases by a factor of ~1.5, in the lower troposphere over the globally averaged value, that is inconsistent with its long chemical lifetime ($\sim 8 \times 10^5$ yr, *e.g.*, Krasnopolsky, 2009) and expected seasonal horizontal meridional circulation that should homogenize any latitudinal variation. Courtin et al. (2015) have confirmed their earlier results that in spite of the seasonal evolution of molecular abundances, temperature, winds in Titan's stratosphere and thermosphere, the polar latitudinal enhancement of the H_2 mole fraction in the northern troposphere persists from winter solstice through spring equinox (see Fig. 8). Based on the long H_2 chemical lifetime, it should be uniformly mixed throughout the troposphere.

Our current understanding of Titan's atmosphere is that hydrogen in atomic and molecular form results from the photochemical conversion of the much more abundant CH_4 into more complex, less saturated hydrocarbons with a net yield of hydrogen. Molecular hydrogen is, for all practical concerns, chemically inert in the atmosphere and production of H_2 is balanced by transport and eventual escape from the atmosphere. This basic framework dates from the pre-Voyager model of Strobel (1974) to the comprehensive post-Voyager model of Yung et al. (1984), and Cassini epoch models (e. g. Lavvas et al., 2008; and Krasnopolsky, 2009). In spite of the increasing complexity of these models, the fact remains that H_2 is chemically inert, for example, Krasnopolsky (2009) finds that the integrated chemical loss of H_2 is only 2% of its integrated production rate.

Throughout most of the atmosphere CH_4 is being irreversibly dissociated by direct photolysis driven principally by the intense solar Lyman α line at 121.6 nm (reaction [2]), indirectly by catalytic C_2H_2 photochemistry [3], and by ion chemistry [1] with net production of H_2, H, and heavy hydrocarbons (Strobel, 2010):

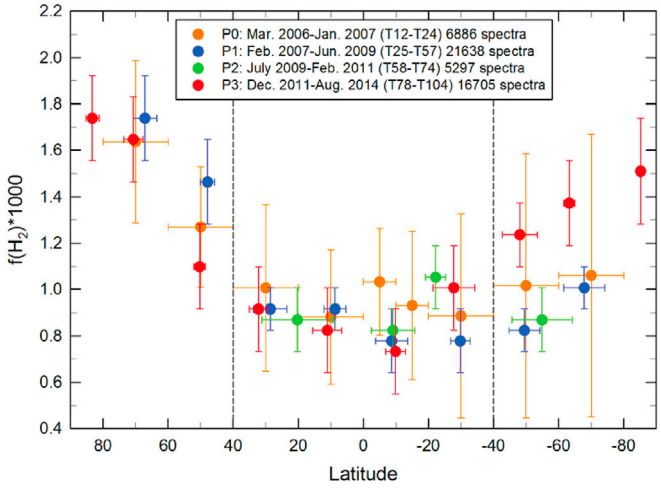

Fig. 8. Latitude distribution of tropospheric H_2 mole fraction in four different time periods extending from March 2006 to August 2014 (adapted from Courtin et al., 2015).

Ionospheric photolysis: $2CH_4 \rightarrow C_2H_2 + 3H_2$ (z~1125 km) (1)

Direct photolysis: $2CH_4 \rightarrow C_2H_4 + 2H_2$ (z~825 km) (2)

Catalytic photolysis: $2CH_4 \rightarrow C_2H_6 + 1H_2$ (z~225 km) (3)

Models with this chemistry require a hydrogen molecular escape rate: $\sim 1.0 \times 10^{28}$ s^{-1}; at the Hunten limiting flux/rate at the homopause; and by enhanced Jeans escape $\sim 1.0 \times 10^{28}$ H_2 s^{-1}) at the exobase. The Jeans escape rate for H_2 is enhanced over the normal Jeans escape rate because the H_2 Jeans λ-parameter (gravitational potential energy/random kinetic energy) is in the range of 2.8–4.8 at the exobase and molecules no longer possess an equilibrium Maxwellian distribution due in part to a non-negligible bulk velocity (cf. Fig. 2, Volkov et al., 2011). As a consequence their convected, distorted distribution function yields an enhanced escape rate (their Fig. 3). Additional production of H_2 (by a factor of 2) beyond conventional chemistry is needed to account for the H_2 mole fraction profile throughout Titan's atmosphere and the additional downward transport of $\sim 1 \times 10^{28}$ H_2 s^{-1} to the troposphere. This additional production must be in the upper atmosphere (Strobel, 2012).

To explain the enhanced H_2 production, Strobel (2010) went to heroic lengths, eventually having to ramp up model parameters to unrealistic extremes. To fit the data, he required (i) that all H atoms in methane were converted to H_2 ($2CH_4 \rightarrow C_2 + 4H_2$), with none going to ethane, ethylene or acetylene; and (ii) the ionospheric ionization rate increased four-fold. However, (i) is chemically implausible and (ii) requires electron densities at least twice those measured. There is no apparent solution that satisfies the two observational constraints on the H_2 mole fraction: 1) in the troposphere and lower stratosphere from the IR measurements of Voyager IRIS and Cassini CIRS of 0.001 and 2) the Cassini INMS measurements of 0.004 in the thermosphere above 950 km.

There is additionally an implied downward net transport of H_2 through the tropopause, which is comparable to the escape rate at the top of the atmosphere ($\sim 1 \times 10^{28}$ s^{-1}). The inferred H_2 latitudinal variation in the troposphere implies much weaker meridional circulation than expected. Instead of seasonal time scales, the implied time scales are ~0.1 Myr = 3400 Saturn years (9000 solar cycles). These may be linked to the "Milankovitch like" cycles invoked by Aharonson et al. (2009) to explain the filled lakes in the northern polar region and empty lake basins at high southern latitudes. This proposed weak circulation is driven by orbital forcing via peak annular insolation differences between the north and south poles over the past 0.2 Myr. In Fig. 3(d) of Aharonson et al. (2009), over the past ~ 150 kyr, more solar radiation has been deposited in the northern polar region than the southern polar region. As a consequence, more stratospheric C_2H_2 catalytic dissociation of CH_4 yields more H_2 production in the northern polar stratosphere consistent with the H_2 latitudinal distribution shown in Fig. 8.

Methane as the precursor of H_2 also has latitudinal variations that are not understood in light of its 30 Myr photochemical lifetime in the stratosphere. Lellouch et al. (2014) found that the CH_4 mole fraction near 15 mbar (~85 km) varied from ~1.0% at low latitudes (in contrast to the Huygens GCMS measurement of 1.48%) and near ±50–55°; to ~1.5% at ±30–35° and polar latitudes. They linked the derived latitudinal variations to convective injection events through the tropopause associated with similar symmetric, latitudinal distributions of tropospheric CH_4 clouds. But 15 mbar is some 40 km above the tropopause and it is hard to comprehend how convection could penetrate that distance into the very stably stratified lower stratosphere. Furthermore, to maintain the measured variations in CH_4 mole fraction, they required a weak meridional circulation with a seasonal time scale on the order of 15 Earth years, but not the "Milankovitch" time scale inferred for H_2. However, both molecules point to slower horizontal mixing times in the troposphere and lower stratosphere.

Given the irreversible nature of CH_4 photochemistry and the deposition of less saturated, more complex hydrocarbons and organic molecules on Titan's surface, it is certainly possible that these hydrocarbons could

recombine with H_2 to reform CH_4 as recombination would be an exothermic process in contrast to the endothermic decomposition of CH_4. The reaction rates would be extremely slow at surface temperatures as one would expect an energy barrier analogous to an activation energy for recombination to occur, unless catalytic elements or minerals are available on Titan's surface to mitigate the energy barrier. It is also interesting to note that the minimum latitudinal H_2 mole fraction values occur within $\pm 30^\circ$ latitude where the organic dunes reside on Titan's surface. Also, the measurements imply that the downward H_2 flow rate to the surface is in substantial excess of the speculative threshold value for methanogenic life consumption of H_2 (McKay and Smith, 2005).

To summarize, key open questions on Titan's hydrogen profile are:

- Why is H_2 flowing down to the surface when there is no known chemical sink there and as a light buoyant molecule loss to space is the obvious loss process?
- Why is its mixing ratio enhanced in the polar regions over the equatorial regions and more in the northern than southern polar regions?
- What is the mechanism for additional hydrogen production in the upper atmosphere?

A combination of future remote-sensing and in situ measurements, with renewed modeling efforts, will be required to understand this problem area more completely.

4.2. Where are all the clouds?

Methane clouds were anticipated to form in Titan's troposphere and were first detected using Earth-based observations (e.g., Toon et al., 1988; Awal and Lunine, 1994; Griffith et al., 1998; Tokano et al., 2001; Lorenz et al., 2005). Given Saturn's obliquity of 26.7° there is a substantial seasonal shift in insolation, and weather patterns are expected to follow solar illumination with Titan's intertropical convergence zone (ITCZ) migrating from one pole to the other near equinox before the atmosphere returns to pole-to-pole circulation (e.g., Mitchell et al., 2006; Tokano, 2008, 2011; Turtle et al., 2011a).

Cassini ISS and VIMS observations of Titan's clouds revealed latitudinal preferences and seasonal changes in Titan's general circulation (Fig. 9A–D) (e.g., Rodriguez et al., 2009, 2011; Turtle et al., 2011a), suggesting that Titan's general circulation is influenced by both sub-seasonal temperature variations of the lower thermal inertia surface and the much longer radiative time scale of Titan's cold, thick troposphere (Turtle et al., 2011a).

At the time of Cassini's arrival in 2004, it was late summer in Titan's southern hemisphere and convective cloud activity was commonly observed near the south pole (Fig. 9 A) (e.g., Porco et al., 2005; Turtle et al., 2011a). In the case of a particularly large cloud outburst in October 2004 (Schaller et al., 2006a), darkening of an extensive area of the surface was subsequently observed to have resulted from rainfall at Arrakis Planitia (Turtle et al., 2009, 2011c). Elongated streaks of clouds several hundred kilometers long, which exhibited convective behavior at small scales (Griffith et al., 2005), were observed consistently at mid-southern latitudes (~40° S) for several years, later becoming common at high northern latitudes (>55° N).

In late 2010, a large storm was observed at low latitudes (Fig. 9E–F), once again resulting in extensive rainfall (Turtle et al., 2011b; Mitchell et al., 2011; Barnes et al., 2013b). However, cloud sightings became rare following the 2010 outburst (Fig. 9), which suggested that enough methane was removed from the atmosphere and the lapse rate was sufficiently stabilized to decrease cloud activity. A similar, shorter, drop in cloud activity followed the 2004 south-polar storm (Fig. 9) (Schaller et al., 2006b; Turtle et al., 2011a). Clouds were expected to pick up with the onset of convection at mid-northern latitudes anticipated in late northern spring. Indeed, most models predicted that this increase would occur well before 2016 (e.g., Rannou et al., 2006; Mitchell, 2008;

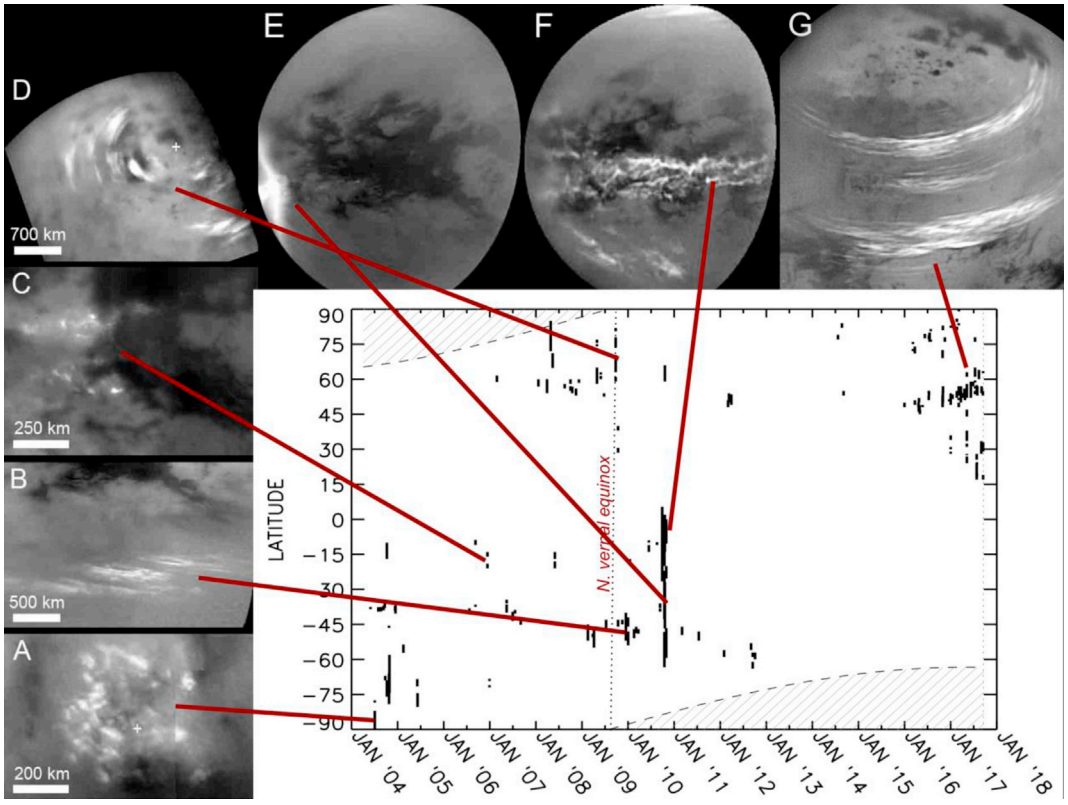

Fig. 9. Cassini ISS images of different types of clouds (A–G) and graph of the latitudes at which clouds have been observed over the mission, spanning May 2004–September 2017 (after Turtle et al., 2017).

Schneider et al., 2012; Lora et al., 2015; Newman et al., 2016).

In 2016, clouds finally began to be observed more regularly at mid-northern latitudes (Fig. 9 G), with isolated cells and more extensive high cirrus detected near the pole, the latter only seen at longer wavelengths (Turtle et al., 2016, 2018). However, Cassini observations through September 2017, ~4 months after the northern summer solstice in May 2017, had not revealed convective storms like those seen at Titan's south pole in 2004 approximately 1.5 years after the southern summer solstice in October 2002. Earth-based observations will continue and hopefully answer the question of when Titan's northern summer storms arrive. Further data analysis (e.g., Corlies et al., 2017; Kelland et al., 2017) and atmospheric modeling, along with future monitoring, will provide important constraints on Titan's atmospheric circulation and its hydrologic cycle, especially outstanding questions about.

- What is the interaction of storms with the north-polar lakes and seas (e.g., Tokano, 2009, 2013)?
- What is the nature of the north-polar cloud features observed by VIMS at 2.1 μm but not by VIMS and ISS at other shorter and longer wavelengths (e.g., Turtle et al., 2016, 2018)?
- What is the distribution of subsurface methane reservoirs (e.g., Lora et al., 2015; Newman et al., 2016)?

4.3. Whence the tilted pole?

The Cassini CIRS instrument (Flasar et al., 2004) measures stratospheric temperature by assuming an abundance of methane, and then adjusting the temperature profile to fit the emission. Longitudinal variations in stratospheric composition and temperature are not expected, due to radiative timescales being significantly longer than the Titan day (Flasar et al., 2014). It was therefore surprising when latitude-longitude maps of 1 mbar temperature taken from 2004 through 2006 showed a strong zonal wavenumber 1 component at northern mid-latitudes. The amplitude and phase of the zonal wavenumber 1 feature were correlated with the meridional temperature gradient, such that the zonal temperature variations were consistent with the temperature field being zonally symmetric about an axis offset relative to the axis of solid body rotation by ~4.1° (Achterberg et al., 2008, Fig. 10), implying through gradient wind balance that the winds are also rotating about an axis offset from the solid body pole. This tilt was later seen in the hemispheric haze asymmetry by Roman et al. (2009), in the stratospheric distribution of HCN by Teanby et al. (2010), and most recently in the zonal winds around the south pole measured by tracking features in the polar cloud that appeared in southern fall (West et al., 2016).

The data of Achterberg et al. (2008) were consistent with the azimuth of the offset being fixed relative to the subsolar longitude, with the north pole tilted towards a point approximately 75° west of the subsolar longitude. This led them to propose that the tilt is the result of feedback between the meridional circulation and the solar forcing, which adjust the spin equator to maximize the efficiency with which the circulation supplies angular momentum to drive the superrotation. Alternately, Tokano (2010) found that his Global Circulation Model (GCM) could produce a tilt from thermal tides. However, using data from a longer time base, Achterberg et al. (2011) found that the longitude of the tilt axis appeared closer to stationary in an inertial (star-fixed) reference frame than in the originally assumed Sun-fixed frame, although the drift in the sun-fixed frame was only weakly significant. The longer time frame now available from Cassini data should resolve if the offset is closer to fixed in an inertial or solar reference frame.

If the offset of the stratospheric rotation axis from the surface pole is fixed in an inertial and not solar reference frame, the mechanisms proposed by Achterberg et al. (2008) and Tokano (2010) are likely incorrect; new mechanisms for producing this offset are needed, as none currently exist. The offset is not seen in those general circulation models of Titan's stratosphere which produce superrotating stratospheric winds comparable to the observations (Newman et al., 2011; Lebonnois et al., 2012; Lora et al., 2015), indicating that our understanding of the processes responsible for the stratospheric circulation are not fully understood. Furthermore, continued monitoring of Titan's stratospheric temperature field, or cloud tracked winds, at spatial resolutions comparable to 2° of arc or less, would allow the measurement of temporal variations in the stratospheric axis offset on timescales longer than a Titan season.

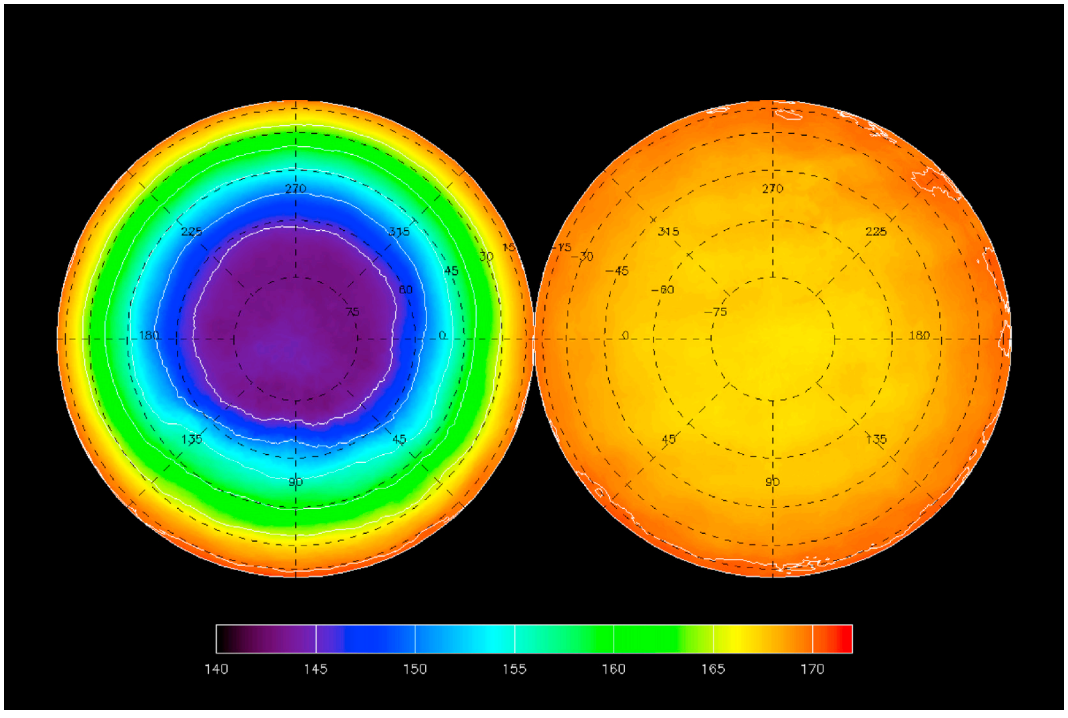

Fig. 10. Temperature contours in Titan's stratosphere at 1 mbar. The apparent axis of symmetry is offset ~4.1° relative to Titan's solid body pole (after Achterberg et al., 2008).

The key open questions for this topic can be summarized as:

- What is the physical mechanism for the offset between Titan's stratospheric and solid body rotation axes?
- Is the offset fixed in magnitude and direction, or does it wander on seasonal or longer time scales?

Further remote-sensing measurements from a Saturn-orbiting, or preferably Titan-orbiting spacecraft, over a time base ultimately spanning a full Titan year or longer will be required to better understand how this phenomenon arises.

4.4. Titan haze

On the eve of the Cassini/Huygens measurements of Titan beginning in 2004, Titan's haze was known to be chemically and spatially complex, with distinct dynamical and chemical regimes: seasonally-changing hemispheric contrasts, polar 'hoods', a 'detached' haze layer at 350 km altitude, and a winter polar cloud feature of unknown composition revealed by spectra at 220 cm^{-1}. Key questions for the Cassini mission included the origin and evolution of the haze particles, the composition(s) of the haze particles, the structure of the haze and what it tells us about processes that determine haze structure (atmospheric circulation, aerosol microphysics), and how the haze influences atmospheric heating/cooling which is important for atmospheric dynamics, chemistry and remote sensing. The Cassini orbiter and Huygens in situ measurements shed light on some of these issues but others remain, and some new puzzles have also emerged.

Titan occupies a special place in the study of planets and satellites in our solar system for many reasons, including the nature of its extensive hydrocarbon/nitrile haze. Although there were hints of the unusual nature of Titan's haze prior to any spacecraft measurements (Veverka, 1973) the first major insights came from Pioneer and Voyager 1 and 2 measurements. The Pioneer 11 Imaging Photopolarimeter experiment (Tomasko and Smith, 1982) revealed strong Rayleigh-like polarization at red and blue wavelengths, the Voyager Photopolarimeter experiment (West et al., 1983) extended wavelength coverage to the near-UV and near-IR and phase angle coverage to 165°. The Voyager images revealed a complex layered structure in the illuminated polar region, a 'detached' haze layer over all latitudes outside of the winter polar haze (Rages and Pollack, 1983), and hemispheric reflectivity asymmetry that Sromovsky et al. (1981) interpreted in terms of a strongly phase-lagged seasonal effect in Titan's stratosphere. The long phase lag derives from a long radiative time constant (relative to the seasonal period) in Titan's stratosphere and troposphere. Images and spectra from the Hubble Space Telescope (Lorenz et al., 2006a, Karkoschka, 2016) and from ground-based telescopes (Ádámkovics et al., 2006) extended measurements of the polar and hemispheric brightness asymmetries to a greater range of wavelengths and a greater span of the seasonal cycle. At thermal-infrared wavelengths the Voyager Infrared Interferometer Spectrometer and Radiometer (IRIS) discovered a broad emission feature at 220 cm^{-1} in the north polar region, thought to be a haze or cloud, but whose composition remains a mystery (Kunde et al., 1981; Coustenis et al., 1999).

Most of the seasonal effects in Titan's haze seen previous to Cassini have also been seen by Cassini instruments, now over a significant fraction of the seasonal cycle. There are several new and unanticipated results from Cassini/Huygens. Briefly, highlights include the discovery of very large negative ions in Titan's high atmosphere (Coates et al., 2007; Waite et al., 2007). This discovery was key to realizing that the initiation of aerosol formation, and the ensuing aerosol particle microphysical processes (Lavvas et al., 2013), was very high up in Titan's atmosphere. The Huygens DISR measured details of Titan's radiation field, including spectra and polarization, from inside the atmosphere and thereby obtained details on the vertical distribution of particles and the aerosol aggregate parameters below 160 km altitude (Tomasko et al., 2008, 2009; Doose et al., 2016). Solar and stellar occultations and limb viewing by Cassini VIMS, the Ultraviolet Imaging Spectrograph (UVIS), and the Composite Infrared Radiometer and Spectrometer (CIRS) provided details on the vertical distribution and composition of aerosol opacity from the ultraviolet to the thermal infrared (Koskinen et al., 2011; Robinson et al., 2014; Vinatier et al., 2010; Anderson and Samuelson, 2011). The CIRS instrument has tracked the evolution of a haze or cloud of unknown composition in the north and south polar stratosphere with a distinctive emission feature seen at 220 cm-1 (Jennings et al., 2015). Recently Anderson et al. (2017) reported a new haze feature at an altitude of 200 km from thermal-infrared limb scans. The ISS and VIMS instruments observed the formation of an HCN ice cloud at 300 km altitude in the southern polar mesosphere after equinox (de Kok et al., 2014; West et al., 2016).

One of Cassini's most recent discoveries is the time evolution of the detached haze. At the very highest spatial resolution (~1 km) many fine layers are visible in the region of the detached haze, but at image scale 5 km/pixel there is one main layer that appears as a local intensity maximum in the images. This layer was seen in Voyager images to be at an altitude of 360 km near the equator and at lower altitude at higher latitude. It extends globally, except in the winter pole above about 55° latitude. Early in the Cassini mission at Saturn (2005–2007) this feature was at 500 km altitude (Porco et al., 2005), but after 2007 its altitude dropped, most rapidly at equinox (West et al., 2011). Fig. 11 shows this behavior. More measurements are now available extending to late in 2016. After a period of no observable detached haze from late 2012 to early 2016, the detached haze is seen to be forming again near 460 km altitude at the equator, but the detection is subtle (West et al., 2017).

The behavior of the detached haze is related to season and, as it is in the mesosphere, the phase lag is short. It is most probably tied to the seasonal behavior of the meridional circulation via vertical and horizontal motion acting on the haze particles. A similar behavior is seen in the general circulation models of Rannou et al. (2002), Lebonnois et al. (2012), and Larson et al. (2015). The meridional circulation in the mesosphere breaks down and reverses near equinox and this is a time of little or no meridional circulation to maintain the haze deficit that produces the appearance of a detached layer.

Some of the most important currently open questions regarding Titan's haze are:

- Does haze control the temperature profile in Titan's high atmosphere as Pluto's haze seems to do (Zhang et al. Nature, 2017)?
- What can we learn from laboratory experiments of haze formation, given the very different boundary conditions (radiation and plasma environment, wall interactions in the laboratory, long time scales for chemical reactions and particle microphysics in the atmosphere but not in the laboratory, atmospheric circulation, etc.)?
- Can we fashion a synthesis of haze results from a variety of instruments on Cassini and other sources which probe different features of the haze?
- How do the photochemical haze and various condensates interact?
- Can we understand the haze well enough to make robust estimates of surface spectral and reflectance distribution properties?
- Is our current picture of haze microphysical processes reasonably complete and correct?

5. Upper atmosphere and interactions

5.1. The origin of complex molecules

Titan harbors one of the richest atmospheric chemistries in the solar system, initiated by the dissociation of the major neutral species (nitrogen and methane) by ultraviolet solar radiation and associated photoelectrons (Lavvas et al., 2011). Before Cassini, it was believed that the particles observed in the stratosphere (i.e. micrometer size organic aerosols) were formed in situ through an intense neutral chemistry

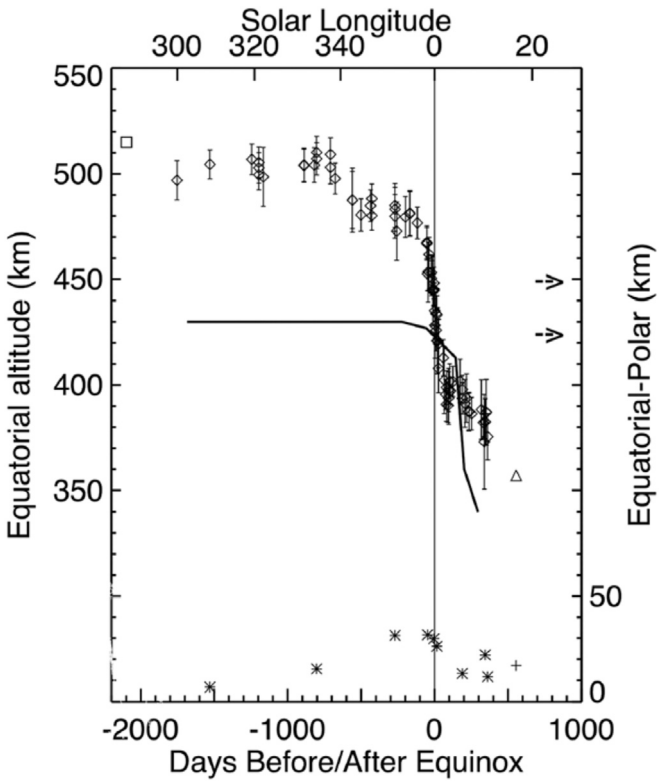

Fig. 11. From West et al. (2011). Measurements from Cassini ISS images of the equatorial altitude of the peak brightness of the detached haze are plotted as diamonds with 1- pixel error bars (left ordinate scale). The triangle at equinox+555 represents Voyager measurements from Rages and Pollack, (1983) who found altitudes from 340 ± 10 to 357 ± 5 km over a range of latitudes with the highest value at the equator and the lowest at the pole. The square at equinox- 2097 days shows the altitude of a strong temperature inversion reported by Sicardy et al. (2006) inferred from stellar occultation data. Two more temperature inversions were reported by Sicardy et al. (1999) from occultation data obtained in 1989 (3413 days after the 1980 equinox at solar longitude 109°) and are indicated by the arrows. The solid curve is the trajectory of the altitu de at the maximum of the detached haze at the equator for the model of Rannou et al., [2002]. Equatorial – polar altitude differences are plotted against the right ordinate scale; the + symbol refers to a measurement by Rages and Pollack (for polar latitude 75° S). The * symbols are measured from Cassini ISS images.

involving complex organic molecules. However, this understanding of Titan's atmospheric chemistry has been strongly challenged by measurements from the Cassini spacecraft. The Ion and Neutral Mass Spectrometer (INMS) and the Cassini Plasma Spectrometer (CAPS) revealed an extraordinary complex ionospheric composition. INMS detected roughly 50 positive ions with m/z < 100 and a density higher than 0.1 cm^{-3} (Waite et al., 2005). CAPS provided evidence for heavy (up to 350 u) positively and negatively charged (up to 4000 u) ions (Coates et al., 2007). These observations indicate that molecular growth starts at much higher altitudes than previously anticipated; triggering a new generation of photochemical/microphysical models (Vuitton et al., 2018) and laboratory experiments (Thissen et al., 2009) in order to put forward new formation processes.

The nature of the lower mass (m/z < 100) positive (Vuitton et al., 2007) and negative (Vuitton et al., 2009) ions detected in the upper atmosphere has been inferred (Fig. 12) and is closely related to the presence of nitrogen-bearing neutrals. Nevertheless, the total positive ion density (essentially $HCNH^+$) and the low mass negative ion densities (CN^-, C_3N^-/C_4H^-) are yet unexplained. Positive ion chemistry contributes to the formation of several molecules (Loison et al., 2015), such as benzene (Vuitton et al., 2008), ammonia (Yelle et al., 2010) and hydrogen isocyanide (Vuitton et al., 2018). Macromolecules (m/z > 100) attach electrons and therefore attract the abundant positive ions, which has been suggested to ultimately lead to the formation of the aerosols (Lavvas et al., 2013). Radiative neutral-neutral association can efficiently form alkanes at altitudes where 3-body collisions are negligible (Vuitton et al., 2012). An incoming flux of oxygen ions from Enceladus activity is likely to be the origin of the observed oxygen-bearing species present in the stratosphere (Hörst et al., 2008), although photochemical models are unable to accurately reproduce their abundances.

New outstanding questions raised by Cassini-Huygens include:

- What is the chemical nature of the macromolecules? Are they nitrogen rich and resemble HCN polymers? Do they contain polyaromatic and/or heterocyclic subunits?
- What are the processes responsible for the growth of the aerosols? What are the relative contributions of ion-neutral vs. radical reaction pathways?
- What is the nature, intensity and time variability of the source(s) of oxygen in the atmosphere? Does it get efficiently incorporated into molecules? Can biological compounds (amino acids, nucleic bases, etc.) or other chemical species with some prebiotic potential be synthesized in the atmosphere?

Another space mission to Titan with a new generation of very-high resolution mass spectrometers (mass resolving power (m/Δm at FWHM) of 100,000 at m/z = 100, sensitivity of 10^{-3} molecule cm^{-3}, mass range up to 1000 u) is required to answer these questions (Briois et al., 2016). The novel measurements should be synergized with state-of-the-art laboratory efforts in order to get some insight into the intermediate steps involved in molecular growth.

5.2. *Titan's escaping methane*

In Titan's upper atmosphere molecular diffusion becomes greater than the eddy diffusion that keeps atmospheric constituents well mixed in the lower atmosphere. This allows species to separate according to their mass and lighter species gradually become more abundant at higher altitudes. The rate of change in the abundance of minor species with increasing altitude can be used to estimate escape rates of that species. However, the type of model used to determine escape rates and the processes assumed to be defining a minor species profile have a major impact on the escape rate derived from observations.

The initial evaluation of methane escape using observations made by Cassini INMS (Waite et al., 2005) and Huygens GCMS (Niemann et al., 2005, 2010) involved the fit of a general diffusion equation to the altitude profile of the methane mixing ratio (Yelle et al., 2006). This study showed that the methane escape flux decreased with increasing eddy diffusion coefficient values. Without any other constraint on eddy diffusion, an estimate for the Jeans escape rate was used to determine a best-fit value.

Following this work, INMS observations showed evidence for a significant population of suprathermal particles suggesting the presence of a corona and significant escape due to sputtering caused by energy deposition into the upper atmosphere (De la Haye et al., 2007). This study used the same basic diffusion equations as Yelle et al. (2006) below 1500 km, but applied the Liouville theorem to observations of the exobase above 1500 km to derive the escape rate. However, a model designed to evaluate hydrodynamic escape of an atmosphere based on the steady state, low Mach number, equations for conservation of mass, momentum and total energy was applied to Titan and suggested escape rates much higher than any previous study had derived (Strobel, 2009). Consistent with the model assumptions, the outflowing CH_4 was subsonic, Mach number <1.

As more observations with INMS became available, further constraints for eddy diffusion were provided. Extensive deconvolution of the INMS mass spectra provided various estimates of the abundance of ^{40}Ar

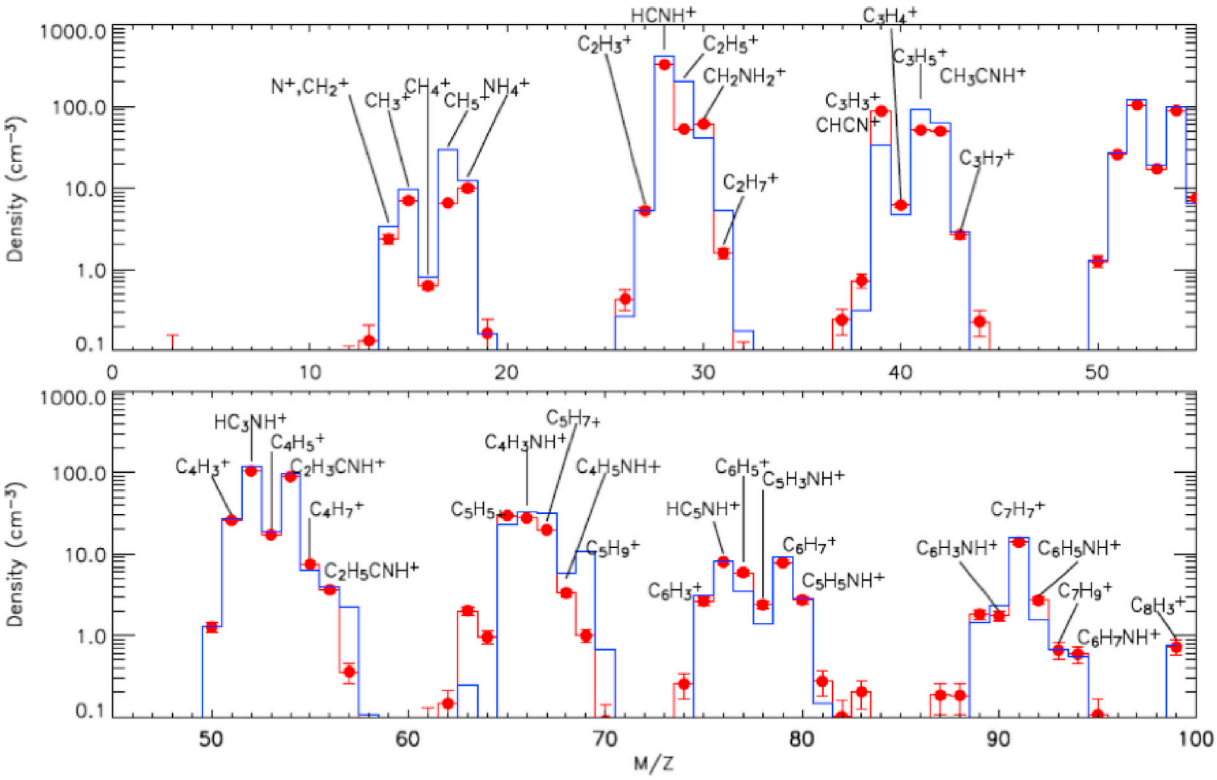

Fig. 12. The red dots show the INMS mass spectrum measured on the T5 flyby, averaged between the altitudes of 1027 and 1200 km. The blue solid line represents a synthetic spectrum generated from an ion chemistry model output with densities of selected neutral species tuned to reproduce the observations. (adapted from Vuitton et al., 2007). (For interpretation of the references to color in this figure legend, the reader is referred to the Web version of this article.)

above 1000 km that could be compared with basic diffusion models with the GCMS abundance near the surface (Yelle et al., 2008). These results suggested much lower eddy diffusion coefficients providing escape rates that were in agreement with the hydrodynamic model results.

A follow up study was then conducted using a three-dimensional global circulation model (3D-GCM) configured to run in one dimension (1D) to provide comparisons to the INMS and GCMS observations (Bell et al., 2010a, 2010b, 2011). This model computed not only the processes evaluated by the basic diffusion model but also energy balance and photochemical production and loss of species. The authors were able to reproduce the results of Strobel (2008) and Yelle et al. (2008) by forcing a high escape rate at the upper boundary (Bell et al., 2010a) but demonstrated that uncertainties in our knowledge of the thermal structure and densities of the upper atmosphere, as well as different possible methods for the analysis of ^{40}Ar led to a wide range of possible methane escape rates that were in agreement with observations (Bell et al., 2010b).

The abundance of ^{40}Ar in the upper atmosphere is particularly problematic. The values derived from INMS measurements can differ by more than 20% between analysis methods and the uncertainty due to counting statistics alone is 25–100%. The authors (Bell et al.) proposed an alternative constraint on eddy diffusion using the INMS and GCMS measurements of ^{14}N/^{15}N in N_2. This provided a range of eddy diffusion coefficients due to variability of the INMS measurements from one flyby to the next. In this model, the eddy diffusion coefficients required to match the nitrogen isotopes were consistently higher, leading to lower escape rates. However, the models of Bell et al. do not start at the surface, nor account for all trace species and isotopes. Therefore, as noted by Strobel (2012), a fully self-consistent model that accounts for all constraints/measurements without high escape rates remains elusive. To date no models have considered that the stratospheric CH_4 mole fraction might be variable with latitude (cf. Section 4.1) and how that impacts the analysis of INMS data.

But not every INMS flyby data set yields the same high CH_4 escape rates. As shown in Table 5 of Cui et al. (2012) and Table 10.1 of Strobel and Cui (2014), occasionally, the CH_4 flux is downward and/or indistinguishable from diffusion equilibrium, although about half of the orbits yielded preferentially strong upward flow of CH_4. Titan's upper atmosphere has shown considerably variability in the CH_4 density profiles and temperature structure inferred from N_2 density profiles from orbit to orbit. Attempts to identify the drivers for this structure variability and inferred CH_4 escape/loss rates yielded larger escape on the nightside over the dayside, whereas magnetospheric lobe-like conditions (factor of 10 reduction in energetic electron flux) yielded diffusive equilibrium, no net CH_4 fluxes (Table 6 in Cui et al., 2012), albeit in the latter case, it is the

Table 1
– Reported methane escape rates, the process assumed to be driving escape, and the models used to derive the escape rates. The term "enforced" is used to specify when the model forces an escape rate at the upper boundary that does not agree with the escape rate self-consistently calculated based on the physical processes included in the model. None of these escape rates imply supersonic outflow.

Escape rate ($cm^{-2}s^{-1}$)	Process	Model used	Reference
$0–2.2 \times 10^9$	Jeans	Basic diffusion	Yelle et al. (2006)
2.8×10^7	Sputtering	Basic diffusion < 1500 km Liouville theorem > 1500 km	De la Haye et al. (2007)
$\sim 2.0 \times 10^9$	Hydrodynamic	Steady state (Ma<1) eqns	Strobel (2009)
$\sim 2.75 \times 10^9$	Hydrodynamic	Basic diffusion	Yelle et al. (2008)
$\sim 2.5 \times 10^9$	Enforced	GCM	Bell et al. (2010a)
$0–2 \times 10^9$	Thermal	GCM	Bell et al. (2010b)

statistics of few flybys. Given this observed variability, 1D models in Table 1 attempted to compute only a single number: the globally averaged, Titan orbit averaged CH_4 escape rate. Reported escape rates for the various published models are summarized in Table 1.

New outstanding questions raised by Cassini-Huygens include:

- Is the single Huygens GCMS observation of ^{40}Ar and $^{14}N/^{15}N$ representative of the values over the entire surface of Titan, or is there spatial variation in these values?
- How does the ^{40}Ar abundance vary spatially in Titan's atmosphere?
- Do aerosols play a role in the loss of CH_4 and other molecules in Titan's atmosphere?

In order to address these questions, a future space mission equipped with a more sensitive mass spectrometer than those on Cassini and Huygens is needed to make measurements at multiple locations on the surface and at various altitudes. The mass spectrometer must have a mass resolution able to separate ^{40}Ar from the hydrocarbons, nitriles and fragments of these species that also appear at mass 40 ($m/\Delta m > 3000$), wide dynamic range (10^{10}), and sensitivity sufficient to detect species at abundances as low as 10^{-8}, with high S/N. A time-of-flight type instrument, instead of a quadrapole as on Cassini-Huygens, would serve well here.

5.3. *The Titan torus mystery: how much is Titan impacting Saturn's magnetosphere?*

Saturn, with its elaborate rings, numerous satellites and dusty plasma, is an evolving planetary system. The effort to understand the inner icy satellites, as well as Titan, the second largest moon in the solar system, and their impacts on their magnetosphere continues to be a significant research focus. Prior to Cassini's arrival at Saturn, analysis of this system relied on limited data gathered from terrestrial and Hubble Space Telescope observations and from three spacecraft (Pioneer 11 and Voyager 1 & 2) that passed through Saturn's magnetosphere. These data indicated both thermal and energetic plasmas composed of a light ion component (protons) and a heavier ion component. Titan's dense nitrogen-rich unprotected atmosphere was proposed as a significant source of particles in Saturn's magnetosphere (Barbosa, 1987; Ip, 1997). These particles were expected to be gravitationally bound to Saturn and thus form a toroidal distribution of co-orbiting particles, or Titan torus. However, these earlier instruments were not able to determine if the heavy ions were oxygen and/or nitrogen, limiting our ability to locate nitrogen sources in the Saturnian system.

Smith et al. (2004) modeled this neutral nitrogen distribution (torus) resulting from Titan's atmospheric loss as well as the spatial distribution of the nitrogen ion source rate in anticipation of Cassini's arrival at Saturn (Fig. 13). Interestingly, they showed that while most of the neutral particles orbited in the outer magnetosphere near Titan's orbit, ionization from this torus is actually more significant in the middle magnetosphere where electron densities and temperatures are more optimized for ionization. They determined that the predicted neutral nitrogen densities were below the detection capabilities of the Cassini Ion and Neutral Mass Spectrometer (INMS) however the pick-up ions generated from this torus should be detectable by the Cassini Plasma Spectrometer (CAPS). Therefore, CAPS data analysis was required for locating nitrogen ions in order to confirm the presence of a neutral nitrogen torus which then provides insight into Titan atmospheric loss.

The arrival of the Cassini spacecraft at Saturn on 1 July 2004 initiated a new era for exploration that is dramatically increasing our understanding of Saturn's magnetosphere. Prior to the discovery of active "jets" emanating from Enceladus' south polar region (Hansen et al., 2006; Porco et al., 2006), Smith et al. (2005) unambiguously discovered nitrogen ions in Saturn's magnetosphere using CAPS data. However, these ions did not appear to be associated with a Titan source but rather exhibited increasing densities with decreasing distance from Enceladus' orbit (Smith et al., 2005). The subsequent detection of active, water ice and gas "jets" emanating from the Enceladus' south polar region possibly containing nitrogen (Waite et al., 2006) confirmed their analysis that Enceladus could indeed be a source of nitrogen for Saturn's magnetosphere. Unfortunately, the Waite et al. (2006) observations did not confirm the presence of N_2 as this detection could be any species with a mass of 28 amu (such as CO or other species fragments). Smith et al. (2007) modeled a possible N_2 plume source showing that 4% N_2 (consistent with Waite et al., 2006) could possibly explain the nitrogen ion observations near Enceladus (observed over the first 15 Cassini orbits). However, more recent UVIS observations indicate <0.5% N_2 in the Enceladus plumes (Hansen et al., 2011). The mechanism for generating these plumes is still being debated partly because at the observed pressure and temperature conditions, water should not exist as a gas. Since ammonia hydrate has a lower melting temperature than water, small amounts of ammonia in the water could conceivably lower the melting point. Thus, ammonia has been suggested as possible volatile species in the plumes. Smith et al. (2008) identified ammonia ion products in the CAPS data (with upper limits on N_2^+) followed by Waite et al. (2009) identifying neutral ammonia in the INMS observations of the plumes at

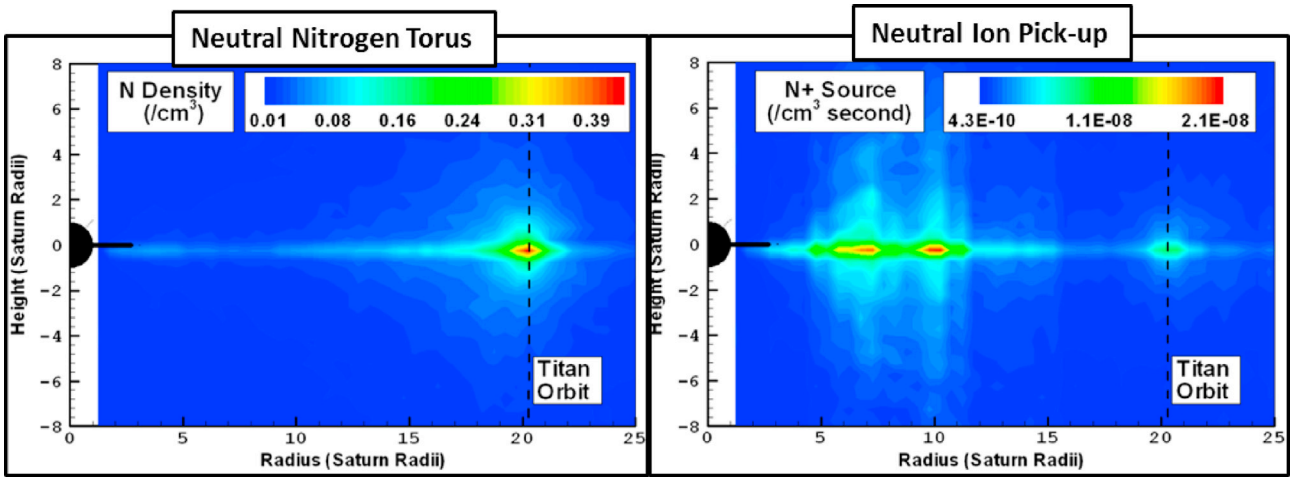

Fig. 13. Pre-Cassini nitrogen distribution models (derived from Smith et al., 2004). Left panel: Neutral N torus (/cm^3) in R vs. Z coordinates (Rs). Right panel: N^+ pick-up ion source from the torus (/sec cm^3) in R & Z coordinates (Rs). Although the peak neutral density is near the source, Titan, peak ion generation is in near the middle magnetosphere where electron densities and temperatures favor ionization. Due to the ambiguity in observations, it is possible this model could still be accurate or the torus may not exist at all.

0.8%. While these observations can provide a source for nitrogen ions in Saturn's magnetosphere, source abundances appear too low to explain amounts of nitrogen ions detected.

However, it is still expected that a dense, unprotected atmosphere such as Titan's should generate a neutral nitrogen torus as predicted. Although the search continues for evidence of a nitrogen torus via ion observations, such evidence remains elusive. In fact, even relatively close to Titan, oxygen ions are observed originating from Enceladus but observations have not been able to positively identity nitrogen ions from Titan. Therefore, the sources of the nitrogen are still unresolved and have a large bearing on our fundamental understanding of Enceladus, Titan, how they interact with the magnetosphere as well the possibility of additional sources. With the significant increase in data and improved analysis techniques, it is now possible to conduct a detailed and comprehensive analysis of the relative nitrogen distribution to better understand sources and dynamics in Saturn's magnetosphere.

In order to gain insight to Titan's interaction with Saturn's magnetosphere, Rymer et al. (2009) found Cassini electron observations that help to identify the specific types of plasma environments that Titan experiences, namely: plasma sheet, lobe-like, magnetosheath, and bimodal plasma. Rymer et al. (2009) analyzed 54 Titan encounters and Smith and Rymer (2014) classified the remaining 20 encounters as well as 118 instances where Cassini crossed Titan's orbit at large distances from Titan. These results allowed for much more accurate modeling of Titan's interaction with Saturn's magnetosphere and also suggest that Titan may be impacting the location of the magnetopause. Additionally, Smith & Rymer (2014) identified a new plasma environment (dense plasma region) that may be caused by a Titan neutral torus.

The above results and preliminary modeling appear to indicate that the Titan torus may actually exist but is difficult to directly detect. In this case, a Titan-generated extended neutral nitrogen torus (similar to the predictions of Smith et al., 2004) may be producing at least some of the nitrogen ions observed by CAPS, and Titan is actually having a larger impact on Saturn's magnetosphere than currently anticipated.

Since we have now detected the torus, the principle question that remains post-Cassini is:

- What are the relative contributions of Enceladus and Titan to the neutral torus?

A neutral mass spectrometer capable of detecting nitrogen densities of $<10\,cm^{-3}$ or an ion mass spectrometer with a larger geometric factor than CAPS could likely resolve this mystery. However, in the absence of such instruments, more advanced data analysis and modeling techniques are required and currently under development to help resolve this Titan Torus mystery.

6. Perspectives – future prospects

Titan is a phenomenologically rich world, with scientific challenges spanning a wide range of disciplines, from organic chemistry, to oceanography, atmospheric dynamics and space physics. The Titan literature has grown at around 100 refereed journal papers per year since Cassini's arrival. Despite this progress, as this review has noted, some questions have not been satisfactorily resolved.

In some cases, this 'unfinished business' is simply a result of limited opportunity – Cassini has been in orbit around Saturn, and its Titan flybys have been brief. Thus only about half of its surface has been mapped with high-quality RADAR imaging, for example, and coverage in the near-infrared has been similarly limited by observation time. Even though Cassini's mission was extended to be more than three times longer than the originally-planned four years, Titan studies could have used much more, and it may be noted that a Titan orbiter (one option for a future mission) would spend longer in close proximity (e.g. <10,000 km altitude) to that world in its first week than has Cassini in all its ~125 flybys. A further limitation is that while Cassini has observed all seasons somewhere on Titan (late summer in the south, northern spring and early summer, early winter in the south etc.) Titan's orbital eccentricity, as well as perhaps geographical differences such as the distribution of surface liquids, means the seasons are not symmetric – as evidenced by the lack of prominent cumulus convection clouds in northern early summer (at present). Observation – from ground-based and space telescopes after Cassini, as well as from future missions to Titan – of late northern summer and southern spring would be valuable.

Other scientific questions were simply out of the reach of Cassini's instrumentation. It was known before Cassini arrived, for example, that interrogating the surface composition by remote sensing would be challenging: most of the visible and infrared spectrum is obscured by the atmosphere, as is all of the ultraviolet. Huygens was (by sheer good luck) able to sample the volatile components of the surface, but only at one location, of what has turned out to be a very diverse surface. Analytic instrumentation, able to measure inorganic as well as a much wider range of organic surface materials, at a range of locations, is a well-established future priority (e.g. Chyba et al., 1999) – this demands either multiple landers, or some sort of mobile – perhaps aerial - platform.

A number of future mission concepts for Titan, embracing an orbiter, fixed or mobile in-situ elements, or both, have been considered in the past, and more than one concept is under present evaluation by NASA. Details are beyond the scope of the present paper (extensive discussion of future exploration are given in e.g. Lorenz, 2000; Coustenis et al., 2009; Barnes et al., 2012; Stofan et al., 2013; Mitri et al., 2018: the broadest discussion is in Leary et al., 2007). Whatever future missions are launched to Titan, it is clear that further spectacular discoveries await.

Acknowledgements

CAN, FMF, RKA and ET acknowledge support by the Cassini–Huygens mission, which is a joint endeavor of NASA, ESA, and ASI and is managed by JPL/Caltech under a contract with NASA. FR acknowledges the support of CNES grants U27 & U45 and thanks ESA for its support as IDS of the Cassini-Huygens mission. Support for this work was provided by a Centre National d'Etudes Spatiales Cassini Participating Scientist grant to V.V. RDL acknowledges the support of NASA grant NNX13AH14G. HTS acknowledges support of the NASA Cassini Data Analysis Program and NASA contract NAS5-97271 Task Order 003. DFS was supported by the Cassini-Huygens Mission through JPL Contract No. 1408487. RL and AS acknowledge the support of NASA grant NNN13D466T under the NASA Cassini Data Analysis Program. Part of this work was carried out at the Jet Propulsion Laboratory, California Institute of Technology, under contract with NASA.

References

Achterberg, R.K., Conrath, B.J., Gierasch, P.J., Flasar, F.M., Nixon, C.A., 2008. Observation of a tilt of Titan's middle-atmospheric superrotation. Icarus 197, 549–555.

Achterberg, R.K., Gierasch, P.J., Conrath, B.J., Flasar, F.M., Nixon, C.A., 2011. Temporal variations of Titan's middle-atmospheric temperatures from 2004 to 2009 observed by Cassini/CIRS. Icarus 211, 686–698.

Ádámkovics, M., de Pater, I., Hartung, M., Eisenhauer, F., Genzel, R., Griffith, C.A., 2006. Titan's bright spots: multiband spectroscopic measurement of surface diversity and hazes. J. Geophys. Res. 111 (E7) https://doi.org/10.1029/2005JE002610. E07S06.

Aharonson, O., Hayes, A.G., Lunine, J.I., Lorenz, R.D., Allison, M.D., Elachi, C., 2009. An asymmetric distribution of lakes on Titan as a possible consequence of orbital forcing. Nat. Geosci. 2, 851–854.

Anderson, C.M., Samuelson, R.E., 2011. Titan's aerosol and stratospheric ice opacities between 18 and 500 μm: vertical and spectral characteristics from Cassini CIRS. Icarus 212, 762–778. https://doi.org/10.1016/j.icarus.2011.01.024.

Anderson, C., et al., 2017. Titan's High Altitude South Polar (HASP) Stratospheric Ice Cloud as Observed by Cassini CIRS. DPS 2017 abstract 304.10, Provo, Utah.

Artemieva, N., Lunine, J., 2003. Cratering on Titan: impact melt, ejecta, and the fate of surface organics. Icarus 164 (2003), 471–480.

Artemieva, N., Lunine, J.I., 2005. Impact cratering on Titan II. Global melt, escaping ejecta, and aqueous alteration of surface organics. Icarus 175 (2), 522–533.

Awal, M., Lunine, J.I., 1994. Moist convective clouds in Titan's atmosphere. Geophys. Res. Lett. 21, 2491–2494.

Barbosa, D.D., 1987. Titan's atomic nitrogen torus: inferred properties and consequences for the Saturnian aurora. Icarus 72, 53–61.

Barnes, J.W., Bow, J., Schwartz, J., Brown, R.H., Soderblom, J.M., Hayes, A.G., Vixie, G., Le Mouélic, S., Rodriguez, S., Sotin, C., Jaumann, R., Stephan, K., Soderblom, L.A., Clark, R.N., Buratti, B.J., Baines, K.H., Nicholson, P.D., 2011. Organic sedimentary deposits in Titan's dry lakebeds: probable evaporate. Icarus 216, 136–140.

Barnes, J.W., Lemke, L., Foch, R., McKay, C.P., Beyer, R.A., Radebaugh, J., Atkinson, D.H., Lorenz, R.D., Le Mouélic, S., Rodriguez, S., Gundlach, J., 2012. AVIATR—aerial vehicle for in-situ and airborne Titan reconnaissance. Exp. Astron. 33 (1), 55–127.

Barnes, Jason, W., Clark, R.N., Sotin, C., Ádámkovics, M., Appéré, T., Rodriguez, S., Soderblom, J.M., Brown, R.H., Buratti, B.J., Baines, K.H., Le Mouélic, S., Nicholson, P.D., 2013a. A transmission spectrum of Titan's north polar atmosphere from a specular reflection of the Sun. Astrophys. J. 777, 161 (12pp).

Barnes, J.W., J Buratti, B., P Turtle, E., Bow, J., Dalba, P.A., Perry, J., Brown, R.H., Rodriguez, S., Le Mouelic, S., Baines, K.H., Sotin, C., Lorenz, R.D., Malaska, M.J., McCord, T.B., N Clark, R., Jaumann, R., Hayne, P.O., Nicholson, P.D., M Soderblom, J., Soderblom, L.A., 2013b. Precipitation-induced surface brightenings seen on Titan by Cassini VIMS and ISS. Plan. Sci. 2.

Beghin, C., Randriamboarison, O., Hamelin, M., Karkoschka, E., Sotin, C., Whitten, R.C., Berthelier, J.-J., Grard, R., Simes, F., 2012. Analytic theory of Titan's Schumann resonance: constraints on ionospheric conductivity and buried water ocean. Icarus 218 (2), 1028–1042.

Bell, J.M., Bougher, S., Waite, J.H., Ridley, A.J., Magee, B.A., Mandt, K.E., Westlake, J., DeJong, A.D., Bar-Nun, A., Jacovi, R., Toth, G., Del La Haye, V., 2010a. Simulating the one-dimensional structure of Titan's upper atmosphere: 1. Formulation of the Titan Global Ionosphere-Thermosphere Model and benchmark simulations. J. Geophys. Res. 115. E12002.

Bell, J.M., Bougher, S., Waite, J.H., Ridley, A.J., Magee, B.A., Mandt, K.E., Westlake, J., De Jong, Del La Haye, V.A.D., Bar-Nun, A., Jacovi, R., Toth, G., Gell, D., Fletcher, G., 2010b. Simulating the one-dimensional structure of Titan's upper atmosphere: 2. Alternative scenarios for methane escape. J. Geophys. Res. 115. E12018.

Bell, J.M., Bougher, S., Waite, J.H., Ridley, A.J., Magee, B.A., Mandt, K.E., Westlake, J., DeJong, A.D., Bar-Nun, A., Jacovi, R., Toth, G., Del La Haye, V., Gell, D., Fletcher, G., 2011. Simulating the one-dimensional structure of Titan's upper atmosphere: 3. Mechanisms determining methane escape. J. Geophys. Res. 116. E11002.

Bills, B.G., Nimmo, F., 2008. Forced obliquity and moments of inertia of Titan. Icarus 196, 293–297.

Bills, B.G., Nimmo, F., 2011. Rotational dynamics and internal structure of Titan. Icarus 214 (2011), 351–355.

Birch, S.P.D., Hayes, A.G., Howard, A.D., Moore, J., Radebaugh, J., 2016. Alluvial fan morphology, distribution, and formation on Titan. Icarus 270, 238–247.

Birch, S.P.D., Hayes, A.G., Dietrich, W.E., Howard, A.D., Bristow, C.S., Malaska, M.J., Moore, J.M., Mastrogiuseppe, M., Hofgartner, J.D., Williams, D.A., White, O.L., Soderblom, J.M., Barnes, J.W., Turtle, E.P., Lunine, J.I., Wood, C.A., Neish, C.D., Kirk, R.L., Stofan, E.R., Lorenz, R.D., Lopes, R.M.C, 2017. Geomorphology of Titan's polar terrains: using landscape form to understand surface processes. Icarus 282, 214–236.

Brassé, C., Buch, A., Coll, P., Raulin, F., 2016. Low temperature alkaline pH hydrolysis of oxygen-free Titan tholins: carbonates Impact. Astrobiology 17 (1), 8–26, 2017.

Briois, C., Thissen, R., Thirkell, L., Aradj, K., Bouabdellah, A., Boukrara, A., Carrasco, N., Chalumeau, G., Chapelon, O., Colin, F., Coll, P., Cottin, H., Engrand, C., Grand, N., Lebreton, J.-P., Orthous-Daunay, F.-R., Pennanech, C., Szopa, C., Vuitton, V., Zapf, P., Makarov, A., 2016. Orbitrap mass analyser for in situ characterisation of planetary environments: performance evaluation of a laboratory prototype. Planet. Space Sci. 131, 33–45.

Brown, R.H., Soderblom, L.A., Soderblom, J.M., Clark, R.N., Jaumann, R., Barnes, J.W., Sotin, C., Buratti, B., Baines, K.H., Nicholson, P.D., 2008. The identification of liquid ethane in Titan's Ontario Lacus. Nature 454, 607–610.

Burr, D.M., Perron, J.T., Lamb, M.P., Irwin, R.P., Collins, G.C., et al., 2013. Fluvial features on Titan: insights from morphology and modeling. Geol. Soc. Am. Bull. 125, 299–321.

Cable, M.L., Hörst, S.M., Hodyss, R., Beauchamp, P.M., Smith, M.A., Willis, P.A., 2012. Titan tholins: simulating Titan organic chemistry in the Cassini-Huygens era. Chem. Rev. 112, 1882–1909.

Cabrol, N.A., Grin, E.A., 2010. Searching for lakes on Mars: four decades of exploration. Lakes on Mars 1–29.

Campbell, D.B., Black, G.J., Carter, L.M., Ostro, S.J., 2003. Radar evidence for liquid surfaces on Titan. Science 302, 431–434.

Castillo-Rogez, J.C., Lunine, J.I., 2010. Evolution of Titan's rocky core constrained by Cassini observations. Geophys. Res. Lett. 37 https://doi.org/10.1029/2010GL044398. L20205.

Choukroun, M., Sotin, C., 2012. Is Titan's shape caused by its meteorology and carbon cycle? Geophys. Res. Lett. 39 https://doi.org/10.1029/2011GL050747. L04201.

Chyba, C., et al., 1999. Europa and Titan: Preliminary Recommendations of the Campaign Science Working Group on Prebiotic Chemistry in the Outer Solar System LPSC XXX Abstract, p. 1537.

Clark, R.N., Curchin, J.M., Hoefen, T.M., Swayze, G.A., 2009. Reflectance spectroscopy of organic compounds I: Alkanes. J. Geophys. Res. C Oceans Atmos. 114 https://doi.org/10.1029/2008JE003150. E03001.

Clark, R.N., Curchin, J.M., Barnes, J.W., Jaumann, R., Soderblom, Larry, Cruikshank, D.P., Brown, R.H., Rodriguez, S., Lunine, J., Stephan, K., Hoefen, T.M., Le Mouelic, S., Sotin, C., Baines, K.H., Buratti, B., Nicholson, P., 2010. Detection and mapping of hydrocarbon deposits on Titan. J. Geophys. Res. 115 https://doi.org/10.1029/2009JE003369. E10005.

Coates, A.J., Crary, F., Lewis, G., Young, D.T., Waite Jr., J.H., Sittler Jr., E.C., 2007. Discovery of heavy negative ions in Titan's ionosphere. Geophys. Res. Lett. 34. L22103.

Coll, P., Navarro-Gonzalez, R., Szopa, C., Poch, O., Ramirez, S.I., Coscia, D., Raulin, F., Cabane, M., Buch, A., Israel, G., 2013. Can laboratory tholins mimic the chemistry producing Titan's aerosols? A review in light of ACP experimental results. Planet. Space Sci. 77, 91–103.

Cordier, D., Mousis, O., Lunine, J.I., Lebonnois, S., Rannou, P., Lavvas, P., Lobo, L.Q., Ferreira, A.G.M., 2012. Titan's lakes chemical composition: sources of uncertainties and variability. Planet. Space Sci. 61, 99–107.

Corlies, P., et al., 2017. Determining Titan's cloud altitude and opacity in the Cassini VIMS dataset. LPSC 48, 2780.

Cornet, T., Bourgeois, O., Le Mouelic, S., Rodriguez, S., Gonzalez, T.L., et al., 2012. Geomorphological significance of Ontario Lacus on Titan: integrated interpretation of Cassini VIMS, ISS and RADAR data and comparison with the Etosha Pan (Namibia). Icarus 218, 788–806.

Courtin, R., Gautier, D., McKay, C.P., 1995. Titan's thermal emission spectrum: reanalysis of the Voyager infrared measurements. Icarus 114, 114–162.

Courtin, R.D., Sim, C., Kim, S., Gautier, D., Jennings, D.E., 2008. Latitudinal variations of tropospheric H_2 on Titan from the Cassini CIRS investigation. In: 40th DPS Meeting Abstract. 31.01, p. 446. Ithaca, (New York), Bull. Amer. Astron. Soc., 40, 31.01.

Courtin, R., Sim, C.K., Kim, S.J., Gautier, D., 2012. The abundance of H_2 in Titan's troposphere from the Cassini CIRS investigation. Planet. Space Sci. https://doi.org/10.1016/j.pss.2012.03.012.

Courtin, R., The CIRS Team, 2015. Seasonal evolution of tropospheric H_2 on Titan from the Cassini CIRS investigation. In: EPSC Abstracts, Vol. 10. EPSC2015–P2089.

Coustenis, A., Schmitt, B., Khanna, B., Trotta, F., 1999. Plausible condensates in Titan's stratosphere from Voyager infrared spectra. Planet. Space Sci. 47, 1305–1329.

Coustenis, A., Atreya, S.K., Balint, T., Brown, R.H., Dougherty, M.K., Ferri, F., Fulchignoni, M., Gautier, D., Gowen, R.A., Griffith, C.A., Gurvits, L.I., Jaumann, R., Langevin, Y., Leese, M.R., Lunine, J.I., McKay, C.P., Moussas, X., Müller-Wodarg, I., Neubauer, F., Owen, T.C., Raulin, F., Sittler, E.C., Sohl, F., Sotin, C., Tobie, G., Tokano, T., Turtle, E.P., Wahlund, J.-E., Waite, J.H., Baines, K.H., Blamont, J., Coates, A.J., Dandouras, I., Krimigis, T., Lellouch, E., Lorenz, R.D., Morse, A., Porco, C.C., Hirtzig, M., Saur, J., Spilker, T., Zarnecki, J.C., Choi, E., Achilleos, N., Amils, R., Annan, P., Atkinson, D.H., Bénilan, Y., Bertucci, C., Bézard, B., Bjoraker, G.L., Blanc, M., Boireau, L., Bouman, J., Cabane, M., Capria, M.T., Chassefière, E., Coll, P., Combes, M., Cooper, J.F., Coradini, A., Crary, F., Cravens, T., Daglis, I.A., de Angelis, E., de Bergh, C., de Pater, I., Dunford, C., Durry, G., Dutuit, O., Fairbrother, D., Flasar, F.M., Fortes, A.D., Frampton, R., Fujimoto, M., Galand, M., Grasset, O., Grott, M., Haltigin, T., Herique, A., Hersant, F., Hussmann, H., Ip, W., Johnson, R., Kallio, E., Kempf, S., Knapmeyer, M., Kofman, W., Koop, R., Kostiuk, T., Krupp, N., Küppers, M., Lammer, H., Lara, L.-M., Lavvas, P., Le Mouélic, S., Lebonnois, S., Ledvina, S., Li, J., Livengood, T.A., Lopes, R.M., Lopez-Moreno, J.-J., Luz, D., Mahaffy, P.R., Mall, U., Martinez-Frias, J., Marty, B., McCord, T., Menor Salvan, C., Milillo, A., Mitchell, D.G., Modolo, R., Mousis, O., Nakamura, M., Neish, C.D., Nixon, C.A., Nna Mvondo, D., Orton, G., Paetzold, M., Pitman, J., Pogrebenko, S., Pollard, W., Prieto-Ballesteros, O., Rannou, P., Reh, K., Richter, L., Robb, F.T., Rodrigo, R., Rodriguez, S., Romani, P., Ruiz Bermejo, M., Sarris, E.T., Schenk, P., Schmitt, B., Schmitz, N., Schulze-Makuch, D., Schwingenschuh, K., Selig, A., Sicardy, B., Soderblom, L., Spilker, L.J., Stam, D., Steele, A., Stephan, K., Strobel, D.F., Szego, K., Szopa, C., Thissen, R., Tomasko, M.G., Toublanc, D., Vali, H., Vardavas, I., Vuitton, V., West, R.A., Yelle, R., Young, E.F., 2009. TandEM: Titan and Enceladus mission. Exp. Astron. 23, 893–946.

Cui, J., Yelle, R.V., Volk, K., 2008. Distribution and escape of molecular hydrogen in Titan's thermosphere and exosphere. J. Geophys. Res. 113. E10004.

Cui, J., Yelle, R.V., Strobel, D.F., Müller-Wodarg, I.C.F., Snowden, D.S., Koskinen, T.T., Galand, M., 2012. The CH_4 structure in Titan's upper atmosphere Revisited. J. Geophys. Res. E11 https://doi.org/10.1029/2012JE004222.

de Kok, Remco J., Teanby, Nicholas A., Maltagliati, Luca, Irwin, Patrick G.J., Vinatier, Sandrine, 2014. HCN ice in Titan's high-altitude southern polar cloud. Nature 514, 65–67. https://doi.org/10.1038/nature13789.

De La Haye, V., Waite Jr., J.H., Johnson, R.E., Yelle, R.V., Cravens, T.E., Luhmann, J.G., Kasprzak, W.T., Gell, D.A., Magee, B., Leblanc, F., Michael, M., Jurac, S., Robertson, I.P., 2007. Cassini Ion and Neutral Mass Spectrometer data in Titan's upper atmosphere and exosphere: observation of a suprathermal corona. J. Geophys. Res. 112. A07309.

Doose, Lyn R., Karkoschka, Erich, Tomasko, Martin G., Anderson, Carrie M., 2016. Vertical structure and optical properties of Titan's aerosols from radiance measurements made inside and outside the atmosphere. Icarus 270, 355–375. https://doi.org/10.1016/j.icarus.2015.09.039.

Dubouloz, N., Raulin, F., Lellouch, E., Gautier, D., 1989. Titan's hypothesized ocean properties : the influence of surface temperature and atmospheric composition uncertainties. Icarus 82, 81–96.

Elachi, C., Allison, M.D., Borgarelli, L., Encrenaz, E., Im, E., Janssen, M.A., Johnson, W.T.K., Kirk, R.L., Lorenz, R.D., Lunine, J.I., Muhleman, D.O., Ostro, S.J., Picardi, G., Posa, F., Rapley, C.G., Roth, L.E., Seu, R., Soderblom, L.A., Vetrell, S., Wall, S.D., Wood, C.A., Zebker, H.A., 2004. RADAR: the Cassini Titan Radar mapper. Space Sci. Rev. 115, 71–110.

Elachi, C., Wall, S., Janssen, M., Stofan, E., Lopes, R., Kirk, R., Lorenz, R., Lunine, J., Paganelli, F., Soderblom, L., Wood, C., Wye, L., Zebker, H., Anderson, Y., Ostro, S., Allison, M., Boehmer, R., Callahan, P., Encrenaz, P., Flamini, E., Francescetti, G., Gim, Y., Hamilton, G., Hensley, S., Johnson, W., Kelleher, K., Muhleman, D., Picardi, G., Posa, F., Roth, L., Seu, R., Shaffer, S., Stiles, B., Vetrella, S., West, R., 2006. Titan Radar mapper observations from Cassini's T3 flyby. Nature 441, 709–713.

Flasar, F.M., 1983. Oceans on Titan? Science 221 (4605), 55–57. https://doi.org/10.1126/science.221.4605.55.

Flasar, F.M., Kunde, V.G., Abbas, M.M., Achterberg, R.K., Ade, P., Barucci, A., Bézard, B., Bjoraker, G.L., Brasunas, J.C., Calcutt, S., Carlson, R., Césarsky, C.J., Conrath, B.J., Coradini, A., Courtin, R., Coustenis, A., Edberg, S., Edgington, S., Ferrari, C., Fouchet, T., Gautier, D., Gierasch, P.J., Grossman, K., Irwin, P., Jennings, D.E., Lellouch, E., Mamoutkine, A.A., Marten, A., Meyer, J.P., Nixon, C.A., Orton, G.S., Owen, T.C., Pearl, J.C., Prangé, R., Raulin, F., Read, P.L., Romani, P.N., Samuelson, R.E., Segura, M.E., Showalter, M.R., Simon-Miller, A.A., Smith, M.D., Spencer, J.R., Spilker, L.J., Taylor, F.W., 2004. Exploring the Saturn system in the thermal infrared: the Composite Infrared sSpectrometer. Space Sci. Rev. 115, 169–297, 2004.

Flasar, F.M., Achterberg, R.K., Schinder, P.J., 2014. Thermal structure of Titan's troposphere and middle atmosphere. In: Müller-Wodarg, Ingo, Griffith, Caitlin A., Lellouch, Emmanuel, Cravens, Thomas E. (Eds.), Titan Interior, Surface, Atmosphere, and Space Environmen, Series: Cambridge Planetary Science (No. 14). Cambridge, 2014.

Ford, D.C., Williams, P.W., 1989a. Karst Geomorphology and Hydrology. Unwin Hyman Ltd, London, p. 601.

Ford, D.C., Williams, P.W., 1989b. Karst Geomorphology and Hydrology. Chapman and Hall, London.

Glein, C.R., Shock, E.L., 2013. A geochemical model of non-ideal solutions in the methane-ethane-propane-nitrogen-acetylene system on Titan. Geochem. Cosmochim. Acta 115, 217–240.

Griffith, C.A., Owen, T., Miller, G.A., Geballe, T., 1998. Transient clouds in Titan's lower atmosphere. Nature 395, 575–578.

Griffith, C.A., Owen, T., Geballe, T., Rayner, J., Rannou, P., 2003. Evidence for the exposure of water ice on Titan's surface. Science 300, 628–630. https://doi.org/10.1126/science.1081897.

Griffith, C.A., Penteado, P., Baines, K., Drossart, P., Barnes, J., Bellucci, G., Bibring, J., Brown, R., Buratti, B., Capaccioni, F., Cerroni, P., Clark, R., Combes, M., Coradini, A., Cruikshank, D., Formisano, V., Jaumann, R., Langevin, Y., Matson, D., McCord, T., Mennella, V., Nelson, R., Nicholson, P., Sicardy, B., Sotin, C., Soderblom, L.A., Kursinski, R., 2005. The evolution of Titan's mid-latitude clouds. Science 310, 474–477.

Griffith, C.A., Penteado, P.F., Turner, J.D., Neish, C.D., Mitri, G., Montiel, M.J., Schoenfeld, A., Lopes, R.M.C., 2017. Titan's Icy Scar, vol. 11. EPSC2017-950, http://meetingorganizer.copernicus.org/EPSC2017/EPSC2017-950.pdf.

Hansen, C.J., Esposito, L., Stewart, A.I.F., Colwell, J., Hendrix, A., Pryor, W., Shemansky, D., West, R., 2006. Enceladus' water vapor plume. Science 311 (5766), 1422–1425.

Hansen, C.J., Shemansky, D.E., Esposito, L.W., Stewart, A.I.F., Lewis, B.R., Colwell, J.E., Hendrix, A.R., West, R.A., Waite Jr., J.H., Teolis, B., Magee, B.A., 2011. The composition and structure of the Enceladus plume. Geophys. Res. Lett. 38 (11) https://doi.org/10.1029/2011GL047415.

Hayes, A.G., 2016. Titan's lakes and seas. Annu. Rev. Earth Planet Sci. 44, 57–83.

Hayes, A., Aharonson, O., Callahan, P., Elachi, C., Gim, Y., Kirk, R., Lewis, K., Lopes, R., Lorenz, R., Lunine, J., Mitchell, K., Mitri, G., Stofan, E., Wall, S., 2008. Hydrocarbon lakes on Titan: distribution and interaction with a porous regolith. Geophys. Res. Lett. 35 (9). L09204.

Hayes, A.G., Wolf, A.S., Aharonson, O., Zebker, H., Lorenz, R., Kirk, R.L., Paillou, P., Lunine, J., Wye, L., Callahan, P., Wall, S., Elachi, C., Hayes, A.G., 2010. Bathymetry and absorptivity of Titan's Ontario Lacus. J. Geophys. Res. C Oceans Atmos. 115 (E9). Available: https://doi.org/10.1029/2009JE003557.

Hayes, A.G., Aharonson, O., Lunine, J.I., Kirk, R.L., Zebker, H.A., Wye, L.C., Lorenz, R.D., Turtle, E.P., Paillou, P., Mitri, G., Wall, S.D., Stofan, E.R., Mitchell, K.L., Elachi, C., Cassini RADAR Team, 2011. Transient surface liquid in Titan's polar regions from Cassini. Icarus 211, 655–671.

Hayes, A.G., Birch, S.P.D., Dietrich, W.E., Howard, A.D., Kirk, R.L., et al., 2017. Topographic constraints on the evolution and connectivity of Titan's lacustrine basins. Geophys. Res. Lett. 44, 11,745–11,753. https://doi.org/10.1002/2017GL075468.

Hayne, P.O., McCord, T.B., Sotin, C., 2014. Titan's surface composition and atmospheric transmission with solar occultation measurements by Cassini VIMS. Icarus 243, 158–172.

Hemingway, D., Nimmo, F., Zebker, H., Iess, L., 2013. A rigid and weathered ice shell on Titan. Nature 500, 550–552.

Hörst, S.M., 2017. Titan's atmosphere and climate. J. Geophys. Res. Planets 122, 432–482. https://doi.org/10.1002/2016JE005240.

Hörst, S.M., Vuitton, V., Yelle, R.V., 2008. The origin of oxygen species in Titan's atmosphere. J. Geophys. Res. 113, E10006.

Iess, L., Rappaport, N., Jacobson, R.A., Racioppa, P., Stevenson, D.J., Tortora, P., Armstrong, J.W., Asmar, S.W., 2010. Gravity field, shape, and moment of inertia of Titan. Science 327, 1367–1369. https://doi.org/10.1126/science.1182583.

Iess, L., Jacobson, R.A., Ducci, M., Stevenson, D.J., Lunine, J.I., Armstrong, J.W., Asmar, S.W., Racioppa, P., Rappaport, N., Tortola, P., 2012. The tides of Titan. Science 337, 457–459. https://doi.org/10.1126/science.1219631.

Ip, W., 1997. On neutral cloud distributions in the Saturnian magnetosphere. Icarus 97, 42–47.

Israel, G., Szopa, C., Raulin, F., Cabane, C., Niemann, H.B., Atreya, S.K., Bauer, S.J., Brun, J.-F., Chassefière, E., Coll, P., Condé, E., Coscia, D., Hauchecorne, A., Millian, P., Nguyen, M.J., Owen, T., Riedler, W., Samuelson, R.E., Siguier, J.-M., Steller, M., Sternberg, R., Vidal-Madjar, C., 2005. Evidence for the presence of complex organic matter in Titan's aerosols by in situ analysis. Nature 438, 796–799, 2005.

Israel, G., Szopa, C., Raulin, F., Cabane, C., Niemann, H.B., Atreya, S.K., Bauer, S.J., Brun, J.-F., Chassefière, E., Coll, P., Condé, E., Coscia, D., Hauchecorne, A., Millian, P., Nguyen, M.J., Owen, T., Riedler, W., Samuelson, R.E., Siguier, J.-M., Steller, M., Sternberg, R., Vidal-Madjar, C., 2006. Astrochemistry: complex organic matter in Titan's aerosols? (Reply). Nature 444 (7119), E6–E7, 2006.

Janssen, M.A., Le Gall, A., Lopes, R.M., Lorenz, R.D., Malaska, M.J., Hayes, A.G., Neish, C.D., Solomonidou, A., Mitchell, K.L., Radebaugh, J., Keihm, S.J., 2016. Titan's surface at 2.18-cm wavelength imaged by the Cassini RADAR radiometer: results and interpretations through the first ten years of observation. Icarus 270, 443–459.

Jennings, Donald, et al., 2015. Evolution of the far-infrared cloud at Titan's south pole. Astrophys. J. Lett. 804 https://doi.org/10.1088/2041-8205/804/2/L34.

Karkoschka, E., 2016. Seasonal variation of Titan's haze at low and high altitudes from HST-STIS spectroscopy. Icarus 270, 339–354.

Kelland, J., Corlies, P., Hayes, A., Rodriguez, S., Turtle, E.P., 2017. Analyzing the dynamic and morphological characteristics of clouds on Titan using the Cassini VIMS dataset. In: American Astronomical Society, DPS Meeting, p. 49 id.304.09.

Khare, B.N., Sagan, C., Ogino, H., Nagy, B., Er, C., Schram, K.H., Arakawa, E.T., 1986. Amino acids derived from Titan tholins. Icarus 68, 176–184.

Kivelson, M.G., Khurana, K.K., Russell, C.T., Walker, R.J., Warnecke, J., Coroniti, F.V., Polanskey, C., Southwood, D.J., Schubert, G., 1996. Discovery of Ganymede's magnetic field by the Galileo spacecraft. Nature 1074 (384), 537–541. https://doi.org/10.1038/384537a0.

Kivelson, M.G., Khurana, K.K., Volwerk, M., 2002. The permanent and inductive magnetic moments of Ganymede. Icarus 157 (2), 507–522. https://doi.org/10.1006/icar.2002.6834.

Kokaly, R.F., Clark, R.N., Swayze, G.A., Livo, K.E., Hoefen, T.M., Pearson, N.C., Wise, R.A., Benzel, W.M., Lowers, H.A., Driscoll, R.L., Klein, A.J., 2017a. USGS Spectral Library Version 7: U.S. Geological Survey Data Series 1035, p. 61. https://doi.org/10.3133/ds1035. https://speclab.cr.usgs.gov/spectral-lib.html.

Kokaly, R.F., Clark, R.N., Swayze, G.A., Livo, K.E., Hoefen, T.M., Pearson, N.C., Wise, R.A., Benzel, W.M., Lowers, H.A., Driscoll, R.L., Klein, A.J., 2017b. USGS Spectral Library Version 7 Data: U.S. Geological Survey Data Release. https://dx.doi.org/10.5066/F7RR1WDJ. https://speclab.cr.usgs.gov/spectral-lib.html.

Korycansky, D.G., Zahnle, K.J., 2005. 2005. Modeling crater populations on Venus and Titan. Planet. Space Sci. 53, 695–710.

Koskinen, T.T., Yelle, R.V., Snowden, D.S., Lavvas, P., Sandel, B.R., Capalbo, F.J., Benilan, Y., West, R.A., 2011. The mesosphere and thermosphere of Titan revealed by Cassini/UVIS stellar occultations. Icarus 507–534. https://doi.org/10.1016/j.icarus.2011.09.022, 216 Pages.

Krasnopolsky, V.A., 2009. A photochemical model of Titan's atmosphere and ionosphere. Icarus 201, 226–256. https://doi.org/10.1016/j.icarus.2008.12.038, 2009.

Krohn, K., Jaumann, R., Stephan, K., Otto, K.A., Schmedemann, N., wagner, R.J., Matz, K.-D., Tosi, F., Zambon, F., Gathen, I., schulzeck, F., Schroder, S.E., Buczkowski, D.L., Hiesinger, H., McSween, H.Y., Pietersm, C.M., Preusker, F., Roatsch, T., Raymond, C.A., Russell, C.T., Williams, D.A., 2016. Cryogenic flow features on Ceres: implications for crater-related cryovolcanism. Geophys. Res. Lett. 23, 11994–12003.

Kunde, V.G., Aikin, A.C., Hanel, R.A., Jennings, D.E., Maguire, W.C., Samuelson, R.E., 1981. C_4H_2, HC_3N and C_2N_2 in Titan's atmosphere. Nature 292, 686.

Larson, Erik J.L., Toon, Owen B., West, Robert A., Friedson, A. James, 2015. Microphysical modeling of Titan's detached haze layer in a 3D GCM. Icarus 254, 122–134. https://doi.org/10.1016/j.icarus.2015.03.010.

Lavvas, P.P., Coustenis, A., Vardavas, I.M., 2008. Coupling photochemistry with haze formation in Titan's atmosphere, Part II: results and validation with Cassini/Huygens data. Planet. Space Sci. 56, 67–99.

Lavvas, P., Galand, M., Yelle, R.V., Heays, A.N., Lewis, B.R., Lewis, G.R., Coates, A.J., 2011. Energy deposition and primary chemical products in Titan's upper atmosphere. Icarus 213, 233–251.

Lavvas, P., Yelle, R.V., Koskinen, T., Bazin, A., Vuitton, V., Vigren, E., Galand, M., Wellbrock, A., Coates, A.J., Wahlund, J.-E., Crary, F.J., Snowden, D., 2013. Aerosol growth in Titan's ionosphere. Proc. Natl. Acad. Sci. Unit. States Am. 110, 2729–2734.

Le Gall, A., Janssen, M.A., Wye, L.C., Hayes, A.G., Radebaugh, J., Savage, C., Zebker, H., Lorenz, R.D., Lunine, J.I., Kirk, R.L., Lopes, R.M.C., Wall, S., Callahan, P., Stofan, E.R., Farr, T., the Cassini Radar Team, 2011. Cassini SAR, radiometry, scatterometry and altimetry over Titan's dune fields. Icarus 213, 608–624.

Le Mouélic, S., Paillou, P., Janssen, M.A., Barnes, J.W., Rodriguez, S., Sotin, C., Brown, R.H., Baines, K.H., Buratti, B.J., Clark, R.N., Crapeau, M., 2008. Mapping and interpretation of Sinlap crater on Titan using Cassini VIMS and RADAR data. J. Geophys. Res.: Plan 113 (E4). https://doi.org/10.1029/2007JE002965. E04003.

Leary, J., Jones, C., Lorenz, R., Strain, R.D., Waite Titan, J.H., August 2007. Explorer NASA Flagship Mission Study. JHU Applied Physics Laboratory public release version. http://www.lpi.usra.edu/opag/Titan_Explorer_Public_Report.pdf. January 2009.

Lebonnois, Sebastien, Burgalat, Jeremie, Rannou, Pascal, Charnay, Benjamin, 2012. Titan global climate model: a new 3-dimensional version of the IPSL Titan GCM. Icarus 218, 707–722. https://doi.org/10.1016/j.icarus.2011.11.032.

Lebreton, J.-P., Matson, D.L., 2002. The Huygens probe: science, payload and mission overview. Space Sci. Rev. 104, 59–100.

Lellouch, E., Bézard, B., Flasar, F.M., Vinatier, S., Achterberg, R., Nixon, C.A., Bjoraker, G.L., Gorius, N., 2014. The distribution of methane in Titan's stratosphere from Cassini/CIRS observations. Icarus 231, 323–337.

Loison, J.C., Hébrard, E., Dobrijevic, M., Hickson, K.M., Caralp, F., Hue, V., Gronoff, G., Venot, O., Bénilan, Y., 2015. The neutral photochemistry of nitriles, amines and imines in the atmosphere of Titan. Icarus 247, 218–247.

Lopes, R.M.C., Mitchell, K.L., Stofan, E.R., Lunine, J.I., Lorenz, R., Paganelli, F., Kirk, R.L., Wood, C.A., Wall, S.D., Robshaw, L.E., Fortes, A.D., Neish, C.D., Radebaugh, J., Reffet, E., Ostro, S.J., Elachi, C., Allison, M.D., Anderson, Y., Boehmer, R., Boubin, G., Callahan, P., Encrenaz, P., Flamini, E., Francescetti, G., Gim, Y., Hamilton, G., Hensley, S., Janssen, M.A., Johnson, W.T.K., Kelleher, K., Muhleman, D.O., Ori, G., Orosei, R., Picardi, G., Posa, F., Roth, L.E., Seu, R., Shaffer, S., Soderblom, L.A.,

Stiles, B., Vetrella, S., West, R.D., Wye, L., Zebker, H.A., 2007. Cryovolcanic features on Titan's surface as revealed by the Cassini Titan Radar mapper. Icarus 186, 395–412.

Lopes, R.M.C., Stofan, E.R., Peckyno, R., Radebaugh, J., Mitchell, K.L., Mitri, G., Wood, C.A., Kirk, R.L., Wall, S.D., Lunine, J.I., Hayes, A., Lorenz, R., Farr, T., Wye, L., Craig, J., Ollerenshaw, R.J., Janssen, M., Le Gall, A., Paganelli, F., West, R., Stiles, B., Callahan, P., Anderson, Y., Valora, P., Soderblom, L., The Cassini RADAR Team, 2010. Distribution and interplay of geologic processes on Titan from Cassini RADAR data. Icarus 205, 540–588. https://doi.org/10.1016/j.icarus.2009.08.010.

Lopes, R.M.C., Kirk, R.L., Mitchell, K.L., Le Gall, A., Barnes, J.W., Hayes, A., Kargel, J., Wye, L., Radebaugh, J., Stofan, E.R., Janssen, M., Neish, C., Wall, S., Wood, C.A., Lunine, J.I., Malaska, M., 2013. Cryovolcanism on Titan: new results from Cassini RADAR and VIMS. J. Geophys. Res. Planets 118, 1–20. https://doi.org/10.1002/jgre.20062.

Lora, J.M., I Lunine, J., Russell, J.L., 2015. GCM simulations of Titan's middle and lower atmosphere and comparison to observations. Icarus 250, 516–528.

Lorenz, R.D., 1993. The surface of Titan in the context of ESA's Huygens Probe. ESA Journal 17, 275–292.

Lorenz, R.D., 1996. Pillow lava on Titan: expectations and constraints on cryovolcanic processes. Planet. Space Sci. 44, 1021–1028.

Lorenz, R.D., 1997. Impacts and cratering on Titan - a pre-Cassini view. Planet. Space Sci. 45, 1009–1019.

Lorenz, R.D., 2000. Post-Cassini exploration of Titan: science rationale and mission concepts. J. Br. Interplanet. Soc. (JBIS) 53 (7/8), 218–234.

Lorenz, R.D., 2017. Wind shear and turbulence on Titan: Huygens analysis. Icarus 295, 119–124.

Lorenz, R.D., Mann, J., 2015. Seakeeping on Ligeia Mare : dynamic response of a floating capsule to waves on the hydrocarbon seas of Saturn's moon Titan. Johns Hopkins APL Tech. Dig. 33 (2), 82–94.

Lorenz, R.D., McKay, C.P., Lunine, J.I., 1997. Photochemically driven collapse of Titan's atmosphere. Science 275, 642.

Lorenz, R.D., Griffith, C.A., Lunine, J.I., McKay, C.P., Renno, N.O., 2005. Convective plumes and the scarcity of Titan's clouds. Geophys. Res. Lett. 32. L01201.

Lorenz, R.D., Lemmon, M.T., Smith, P.H., 2006a. Seasonal evolution of Titan's dark polar hood: midsummer disappearance observed by the Hubble Space Telescope. Mon. Not. Roy. Astron. Soc. 369, 1683–1687. https://doi.org/10.1111/j.1365-2966.2006.10405.x.

Lorenz, R.D., Wall, S., Radebaugh, J., Boubin, G., Reffet, E., Janssen, M., Stofan, E., Lopes, R., Kirk, R., Elachi, C., Lunine, J., Mitchell, K., Paganelli, F., Soderblom, L., Wood, C., Wye, L., Zebker, H., Anderson, Y., Ostro, S., Allison, M., Boehmer, R., Callahan, P., Encrenaz, P., Ori, G.G., Francescetti, G., Gim, Y., Hamilton, G., Hensley, S., Johnson, W., Kelleher, K., Muhleman, D., Picardi, G., Posa, F., Roth, L., Seu, R., Shaffer, S., Stiles, B., Vetrella, S., Flamini, E., West, R., 2006b. The sand seas of Titan: Cassini RADAR observations of longitudinal dunes. Science 312, 724.

Lorenz, R.D., Wood, C.A., Lunine, J.I., Wall, S.D., Lopes, R.M., Mitchell, K.L., Paganelli, F., Anderson, Y.Z., Wye, L., Tsai, C., Zebker, H., Stofan, E.R., 2007. Titan's young surface: initial impact crater survey by Cassini RADAR and model comparison. Geophys. Res. Lett. 34. L07204.

Lorenz, Ralph D., Mitchell, Karl L., Kirk, Randolph L., Hayes, Alexander G., Aharonson, Oded, Zebker, Howard A., Paillou, Phillipe, Radebaugh, Jani, Lunine, Jonathan I., Janssen, Michael A., Wall, Stephen D., Lopes, Rosaly M., Stiles, Bryan, Ostro, Steve, Mitri, Giuseppe, Stofan, Ellen R., 2008. Titan's inventory of organic surface materials. Geophys. Res. Lett. 35.

Lunine, J.I.R.D., Lorenz, R.D., 2009. Rivers, lakes, dunes and rain: crustal processes in Titan's methane cycle. Annu. Rev. Earth Planet Sci. 37, 299–301.

Lunine, J.I., Rizk, B., 1989. Thermal evolution of Titan's atmosphere. Icarus 80, 370–389.

Lunine, J.I., Stevenson, D.J., 1985. Evolution of Titan's coupled ocean-atmopshere system and interaction of ocean with bed-rock. In: Klinger, J., et al. (Eds.), Ices in the Solar System, pp. 741–757 (Reidel, Dordrecht).

Lunine, J.I., Stevenson, D.J., Yung, Y.L., 1983. Ethane ocean on Titan? Science 222, 1229–1230.

MacKenzie, S.M., Barnes, J.W., Sotin, C., Soderblom, J.M., Le Mouelic, S., et al., 2014. Evidence of Titan's climate history from evaporite distribution. Icarus 243, 191–207.

Mandt, K.E., Waite, J.H., Teolis, B., Magee, B.A., Bell, J., Westlake, J.H., Nixon, C.A., Mousis, O., Lunine, J.I., 2012. The $^{12}C/^{13}C$ ratio on Titan from Cassini INMS measurements and implications for the evolution of methane. Astrophys. J. 749 (2), 160, 14.

Mastrogiuseppe, M., Hayes, A.G., Poggiali, V., Lunine, J.I., Lorenz, R.D., Seu, R., Le Gall, A., Notarnicola, C., Mitchell, K.L., Malaska, M., Birch, S.P.D., 2018. Bathymetry and composition of Titan's Ontario Lacus derived from Monte Carlo-based waveform inversion of Cassini RADAR altimetry data. Icarus 300, 203–209. ISSN 0019–1035.

Mastrogiuseppe, M., Poggiali, V., Hayes, A., Lorenz, R., Lunine, J., Picardi, G., Seu, R., Flamini, E., Mitri, G., Notarnicola, C., Paillou, P., Zebker, H., 2014. The bathymetry of a Titan sea. Geophys. Res. Lett. [Online] 41 (5), 1432–1437. Available: https://doi.org/10.1002/2013GL058618.

Mastrogiuseppe, M., et al., Geoscience and Remote Sensing, IEEE, 2016. Radar Sounding Using the Cassini RADAR Altimeter: Waveform Modeling and Monte Carlo Approach for Inversion of Observations of Titan's Seas.

Matson, D.L., Spilker, L.J., Lebreton, J.-P., 2002. The Cassini-Huygens mission to the Saturn system. Space Sci. Rev. 104, 1–58, 2002.

McKay, C.P., Smith, H.D., 2005. Possibilities for methanogenic life in liquid methane on the surface of Titan. Icarus 178, 274–276. https://doi.org/10.1016/j.icarus.2005.05.018.

Michaelides, R.J., Hayes, A.G., Mastrogiuseppe, M., Zebker, H.A., Farr, T.G., Malaska, M.J., Poggiali, V., Mullen, J.P., 2016. Constraining the physical properties of Titan's empty lake basins using nadir and off-nadir Cassini RADAR backscatter. Icarus 270, 57–66.

Mitchell, J.L., 2008. The drying of Titan's dunes: Titan's methane hydrology and its impact on atmospheric circulation. J. Geophys. Res. 113, E08015.

Mitchell, J., Pierrehumbert, R., Frierson, D., Caballero, R., 2006. The dynamics behind Titan's methane clouds. Proc. Natl. Acad. Sci. Unit. States Am. 103, 18,421–18,426.

Mitchell, K.L., Lopes, R.M.C., Radebaugh, J., Lorenz, R.D., Stofan, E.R., et al., 2008. The formation of high latitude Karst lakes on Titan and implications for the existence of polar caps. In: Lunar and Planetary Science Conference, p. 2170.

Mitchell, J.L., Ádámkovics, M., Caballero, R., Turtle, E.P., 2011. Locally enhanced precipitation organized by planetary-scale waves on Titan. Nat. Geosci. 4, 589–592.

Mitchell, K.L., et al., 2015. Laboratory measurements of cryogenic liquid alkane microwave absorptivity and implications for the composition of Ligeia Mare, Titan. Geophys. Res. Lett. 42, 1340–1345. https://doi.org/10.1002/2014GL059475.

Mitri, G., Meriggiola, R., Hayes, A., Lefevre, A., Tobie, G., Genova, A., Lunine, J.I., Zebker, H., 2014. Shape, topography, gravity anomalies and tidal deformation of Titan. Icarus 236, 169–177. https://doi.org/10.1016/j/Icarus.2014.03.018.

Mitri, G., Postberg, F., Soderblom, J.M., Wurz, P., Tortora, P., Abel, B., Barnes, J.W., Berga, M., Carrasco, N., Coustenis, A., de Vera, J.P.P., 2018. Explorer of Enceladus and Titan (E^2T): investigating ocean worlds' evolution and habitability in the solar system. Planet. Space Sci. submitted.

Moore, J.M., Howard, A.D., 2010. Are the basins of Titan's Hotei and Tui Regio sites of former low latitude seas? Geophys. Res. Lett. 37 https://doi.org/10.1029/2010GL045234. L22205.

Moore, J.M., Pappalardo, R.T., 2011. Titan: an exogenic world? Icarus 212, 790–806.

Moore, J.M., et al., 2016. The geology of Pluto and charon through the eyes of New Horizons. Science 351, 1284–1293.

Neish, C.D., Lorenz, R.D., 2012. Titan's global crater population: a new assessment. Planet. Space Sci. 60, 26–33.

Neish, C.D., Lorenz, R.D., 2014. Elevation distribution of Titan's craters suggests extensive wetlands. Icarus 228, 27–34.

Neish, C.D., Somogyi, A., Smith, M.A., 2009. Low temperature hydrolysis of laboratory tholins in ammonia-water solutions: implications for prebiotic chemistry on Titan. Icarus 201, 412–421.

Neish, C.D., Somogyi, A., Lunine, J.I., Smith, M.A., 2010. Titan's primordial soup: formation of amino acids via low-temperature hydrolysis of tholins. Astrobiology 10, 337–347.

Neish, C.D., Barnes, J.W., Sotin, C., MacKenzie, S., Soderblom, J.M., Le Mouélic, S., Kirk, R.L., Stiles, B.W., Malaska, M.J., Le Gall, A., Brown, R.H., 2015. Spectral properties of Titan's impact craters imply chemical weathering of its surface. Geophys. Res. Lett. 42 (10), 3746–3754.

Nelson, R.M., Kamp, L.W., Matson, D.L., Irwin, P.G.J., Baines, K.H., Boryta, M.D., Leader, F.E., Jaumann, R., Smythe, W.D., Sotin, C., Clark, R.N., Cruikshank, D.P., Drossart, P., Pearl, J.C., Hapke, B.W., Lunine, J., Combes, M., Bellucci, G., Bibring, J.-P., Capaccioni, F., Cerroni, P., Coradini, A., Formisano, V., Filacchione, G., Langevin, R.Y., McCordo, T.B., Mennella, V., Nicholson, P.D., Sicardy, B., 2009a. Saturn's Titan: surface change, ammonia, and implications for atmospheric and tectonic activity. Icarus 199, 429–441. https://doi.org/10.1016/j.icarus.2008.08.013.

Nelson, R.M., Kamp, L.W., Lopes, R.M.C., Matson, D.L., Kirk, R.L., Hapke, B.W., Wall, S.D., Boryta, M.D., Leader, F.E., Smythe, W.D., Mitchell, K.L., Baines, K.H., Jaumann, R., Sotin, C., Clark, R.N., Cruikshank, D.P., Drossart, P., Lunine, J.I., Combes, M., Bellucci, G., Bibring, J.-P., Capaccioni, F., Cerroni, P., Coradini, A., Formisano, V., Filacchione, G., Langevin, Y., McCord, T.B., Mennella, V., Nicholson, P.D., Sicardy, B., Irwin, P.G.J., 2009b. Photometric changes on Saturn's moon Titan: evidence for cryovolcanism. Geophys. Res. Lett. 36 https://doi.org/10.1029/2008GL036206. L04202.

Newman, C.E., Lee, C., Lian, Y., Richardson, M.I., Toigo, A.D., 2011. Stratospheric superrotation in the TitanWRF model. Icarus 213, 636–654.

Newman, C.E., et al., 2016. Simulating Titan's methane cycle with the TitanWRF general circulation model. Icarus 267, 106–134.

Niemann, H.B., Atreya, S.K., Bauer, S.J., Carignan, G.R., Demick, J.E., Frost, R.L., Gautier, D., Haberman, J.A., Harpold, D.N., Hunten, D.M., Israel, G., Lunine, J.I., Kasprzak, W.T., Owen, T.C., Paulkovich, M., Raulin, F., Raaen, E., Way, S.H., 2005. The abundances of constituents of Titan's atmosphere from the GCMS instrument on the Huygens probe. Nature 438, 779–784. https://doi.org/10.1038/nature04122.

Niemann, H.B., Atreya, S.K., Demick, J.E., et al., 2010. Composition of Titan's lower atmosphere and simple surface volatiles as measured by the Cassini-Huygens probe gas chromatograph mass spectrometer experiment. J. Geophys. Res. 115. E12006, 2010.

Nimmo, F., Bills, B.G., 2010. Shell thickness variations and the long-wavelength topography of Titan. Icarus 208 (2010), 896–904.

Nixon, C.A., Temelso, B., Vinatier, S., Teanby, N.A., Bézard, B., Achterberg, R.K., Mandt, K.E., Sherrill, C.D., Irwin, P.G.J., Jennings, D.E., Romani, P.N., Coustenis, A., Flasar, F.M., 2012. Isotopic ratios in Titan's methane: measurements and modeling. Astrophys. J. 749 (2), 159, 15.

Nixon, C.A., Achterberg, R.K., Ádámkovics, M., Bézard, B., Bjoraker, G.L., Cornet, T., Hayes, A.G., Lellouch, E., Lemmon, M.T., López-Puertas, M., Rodriguez, S., Sotin, C., Teanby, N.A., Turtle, E.P., West, R.A., 2016. Titan science with the James Webb Space Telescope. Publ. Astron. Soc. Pac. 128 (959), 018007.

Owen, T., 1985. Life as a planetary phenomenon. Orig. Life 15, 221–234.

Perron, J.T., Lamb, M.P., Koven, C.D., Fung, I.Y., Yager, E., Adamkovics, M., 2006. Valley formation and methane precipitation rates on Titan. Journal of Geophysical Research-Planets 111.

Poch, O., Coll, P., Buch, A., Ramirez, S.I., Raulin, F., 2012. Production yields of organics of astrobiological interest from H_2O-NH_3 hydrolysis of Titan's tholins. Planet. Space Sci. 61, 114–123.
Porco, C., et al., 2005. Imaging of Titan from the Cassini spacecraft. Nature 434, 159–168. https://doi.org/10.1038/nature03436.
Porco, C.C., 24 colleagues, 2006. Cassini observes the active south pole of Enceladus. Science 311 (5766), 1393–1401.
Rages, K., Pollack, J.B., 1983. Vertical distribution of scattering hazes in Titan's upper atmosphere. Icarus 55, 50–62. https://doi.org/10.1016/0019-1035(83)90049-0.
Ramirez, S.I., Coll, P., Buch, A., Brasse, C., Poch, O., Raulin, F., 2010. The fate of aerosols on the surface of Titan. Faraday Discuss 147, 419–427.
Rannou, P., Hourdin, F., McKay, C.P., 2002. A wind origin for Titan's haze structure. Nature 418, 853–856. https://doi.org/10.1038/nature00961.
Rannou, P., Montmessin, F., Hourdin, F., Lebennois, S., 2006. The latitudinal distribution of clouds on Titan. Science 311, 201–205.
Raulin, F., Owen, T., 2002. Organic chemistry and exobiology on Titan. Space Sci. Rev. 104 (1–2), 379–395.
Raulin, F., Brassé, C., Poch, O., Coll, P., 2012. Prebiotic-like chemistry on Titan. Chem. Soc. Rev. 41 (16), 5380–5393.
Robinson, Tyler D., Maltagliati, Luca, Marley, Mark S., Fortney, Jonathan J., 2014. Titan solar occultation observations reveal transit spectra of a hazy world. Proc. Natl. Acad. Sci. U.S.A. 111, 9042–9047. https://doi.org/10.1073/pnas.1403473111.
Rodriguez, S., et al., 2009. Global circulation as the main source of cloud activity on Titan. Nature 459, 678–682.
Rodriguez, et al., 2011. Titan's cloud seasonal activity from winter to spring with Cassini/VIMS. Icarus 216, 89–110.
Rodriguez, S., Maltagliati, L., Sotin, C., Rannou, P., Bézard, B., Cornet, T., 2016. A new description of Titan's aerosol optical properties from the analysis of VIMS Emission Phase Function observations. In: American Astronomical Society, DPS Meeting, p. 48 id.424.03.
Roman, M.T., West, R.A., Banfield, D.J., Gierasch, P.J., Achterberg, R.K., Nixon, C.A., Thomas, P.C., 2009. Determining a tilt in Titan's north-south albedo asymmetry from Cassini images. Icarus 203, 242–249.
Ruesch, O., Platz, T., Schenk, P., McFadden, L.A., Castillo-Rogez, J.C., Quick, L.C., Byrne, S., Preusker, F., O'Brien, D.P., Schmedemann, N., Williams, D.A., Li, J.-Y., Bland, T., Hiesinger, Kneissl, T., Schaefer, Neesemann, Pasckert, H., Schmidt, E., Sykes, M.V., Nathues, Roatsch, A., Hoffmann, M., Raymond, C.A., Russell, C.T., 2016. Cryovolcanism on Ceres. Science 353, 4286.
Rymer, A.M., Smith, H.T., Wellbrock, A., Coates, A.J., Young, D.T., 2009. Discrete classification and electron energy spectra of Titan's varied magnetospheric environment. Geophys. Res. Lett. 36 (15) https://doi.org/10.1029/2009GL039427.
Sagan, C., Dermott, S.F., 1982. The tide in the seas of Titan. Nature 300, 731–733.
Sagan, C., Khare, B.N., 1979. Tholins: organic chemistry of interstellar grains and gas. Nature 277, 102–107.
Samuelson, R.E., Nath, N.R., Borysow, A., 1997. Gaseous abundances and methane supersaturation in Titan's troposphere. Planet. Space Sci. 45, 959–980.
Saur, J., Duling, S., Roth, L., Jia, X., Strobel, D.F., Feldman, P.D., Christensen, U.R., Retherford, K.D., McGrath, M.A., Musacchio, F., Wennmacher, A., Neubauer, F.M., Simon, S., Hartkorn, O., 2015. The search for a subsurface ocean in Ganymede with Hubble Space Telescope observations of its auroral ovals. J. Geophys. Res. Space Physics 120 (3), 1715–1737. https://doi.org/10.1002/2014JA020778.
Schaller, E., Brown, M., Roe, H., Bouchez, A., 2006a. A large cloud outburst at Titan's South Pole. Icarus 182, 224–229.
Schaller, E., et al., 2006b. Dissipation of Titan's south polar clouds. Icarus 184, 517–523.
Schneider, T., et al., 2012. Polar methane accumulation and rainstorms on Titan from simulations of the methane cycle. Nature 481, 58–61.
Sicardy, B., et al., 1999. The structure of Titan's stratosphere from the 28 Sgr occultation. Icarus 142 (2), 357–390.
Sicardy, B., et al., 2006. The two Titan stellar occultations of 14 November 2003. J. Geophys. Res. 111. E11S91.
Smith, H.T., Rymer, A.M., 2014. An empirical model for the plasma environment along Titan's orbit based on Cassini plasma observations. J. Geophys. Res. 119.
Smith, P.H., Lemmon, M.T., Lorenz, R.D., Sromovsky, L.A., Caldwell, J.J., Allison, M.D., 1996. Titan's surface, revealed by HST imaging. Icarus 119, 336–349. https://doi.org/10.1006/icar.1996.0023.
Smith, H.T., Johnson, R.E., Shematovich, V.I., 2004. Titan's atomic and molecular nitrogen tori. Geophys. Res. Lett. 31 (16) https://doi.org/10.1029/2004GL020580. L16804.
Smith, H.T., et al., 2005. Discovery of nitrogen in Saturn's inner magnetosphere. Geophys. Res. Lett. 32 (14) https://doi.org/10.1029/2005GL022654. L14S03.
Smith, H.T., et al., 2007. Enceladus: the likely dominant nitrogen source in Saturn's magnetosphere. Icarus 188 (2), 356–366. https://doi.org/10.1016/j.icarus.2006.12.007.
Smith, H.T., et al., 2008. Enceladus: a potential source of ammonia products and molecular nitrogen for Saturn's magnetosphere. J. Geophys. Res. https://doi.org/10.1029/2008JA013352.
Soderblom, L.A., et al., 2009. The geology of Hotei Regio, Titan: Correlation of Cassini VIMS and RADAR. Icarus 204, 610–618.
Soderblom, J.M., Brown, R.H., Soderblom, L.A., Barnes, J.W., Jaumann, R., Le Mouélic, S., Sotin, C., Stephan, K., Baines, K.H., Buratti, B.J., Clark, R.N., 2010. Geology of the selk crater region on Titan from Cassini VIMS observations. Icarus 208 (2), 905–912.
Sohl, F., et al., 2014. Structural and tidal models of Titan and inferences on cryovolcanism. J. Geophys. Res. Planets 119 (5), 1013–1036.
Solomonidou, A., Coustenis, A., Hirtzig, M., Rodriguez, S., Stephan, K., Lopes, R.M.C., Drossart, P., Sotin, C., Le Mouélic, S., Lawrence, K., Bratsolis, E., Jaumann, R., Brown, R.H., 2016. Temporal variations of Titan's surface with Cassini/VIMS. Icarus 270, 85–99.
Solomonidou, A., Coustenis, A., Lopes, R.M.C., Malaska, M.J., Rodriguez, S., Drossart, P., Elachi, C., Schmitt, B., Philippe, S., Janssen, M., Hirtzig, M., Wall, S., Sotin, C., Lawrence, K., Altobelli, N., Bratsolis, E., Radebaugh, J., Stephan, K., Brown, R.H., Le Mouelic, S., Le Gall, A., Villanueva, E.V., Brossier, J.F., Bloom, A.A., Witasse, O., Matsoukas, C., Schoenfeld, A., 2018. The spectral nature of Titan's major geomorphological units: constraints on surface composition. J. Geophys. Res. Planets. https://doi.org/10.1002/2017JE005477 (in press).
Sotin, C., Kalousova, K., 2016. Evolution of Titan's High-pressure Ice Layer. American Geophysical Union. Fall General Assembly 2016, #P33F-02.
Sotin, C., Jaunmann, R., Buratti, B.J., Brown, R.H., Clark, R.N., Soderblom, L.A., Baines, K.H., Bellucci, G., Bribing, J.-P., Capaccioni, F., Cerroni, P., Coradini, A., Cruikshank, D.P., Drossart, P., Formisano, V., Langevin, Y., Matson, D.L., McCord, T.B., Nelson, R.M., Nicholson, P.D., Sicardy, B., Le Mouelic, S., Rodriguez, S., Stephan, K., Scholz, C.K., 2005. Release of volatiles from a possible cryovolcano from near-infrared imaging of Titan. Nature 435, 786–789.
Sotin, C., Lawrence, K.J., Reinhardt, B., Barnes, J.W., Brown, R.H., Hayes, A.G., Le Mouélic, S., Rodriguez, S., Soderblom, J.M., Soderblom, L.A., Baines, K.H., Buratti, B.J., Clark, R.N., Jaumann, R., Nicholson, P.D., Stephan, K., 2012. Observations of Titan's Northern lakes at 5 lm: implications for the organic cycle and geology. Icarus 221, 768–786.
Sromovsky, L.A., Suomi, V.E., Pollack, J.B., Krauss, R.J., Limaye, S.S., Owen, T., Revercomb, H.E., Sagan, C., 1981. Implications of Titan's north-south brightness asymmetry. Nature 292, 698–702. https://doi.org/10.1038/292698a0.
Stofan, E.R., Elachi, C., Lunine, J.I., Lorenz, R.D., Stiles, B., et al., 2007. The lakes of Titan. Nature 445, 61–64.
Stofan, et al., 2013. TiME- the Titan Mare Explorer. In: IEEE Aerospace Conference.
Strobel, D.F., 1974. The photochemistry of hydrocarbons in Titan's atmosphere. Icarus 21, 466–470.
Strobel, D.F., 1982. Chemistry and evolution of Titan's atmosphere. Planet. Space Sci. 30 (8), 839–848.
Strobel, D.F., 2008. Titan's hydrodynamically escaping atmosphere. Icarus 193, 588–594.
Strobel, D.F., 2009. Titan's hydrodynamically escaping atmosphere: escape rates and the structure of the exobase region. Icarus 202, 632–641.
Strobel, D.F., 2010. Molecular hydrogen in Titan's atmosphere: implications of the measured tropospheric and thermospheric mole fractions. Icarus 208, 878–886.
Strobel, D.F., 2012. Hydrogen and methane in Titan's atmosphere: chemistry, diffusion, escape, and the Hunten limiting flux principle. Can. J. Phys. 90, 795–805.
Strobel, D.F., Cui, J., 2014. Titan's upper atmosphere/exosphere, escape processes and rates. In: Mueller-Wodarg, I., Griffith, C., Lellouch, E., Cravens, T. (Eds.), Titan: Interior, Surface, Atmosphere and Space Environment. Cambridge University Press/Cambridge Planetary Science Series, pp. 355–375.
Tan, S.P., Kargel, J.S., Jennings, D.E., Mastrogiuseppe, M., Adidharma, H., Marion, G.M., 2015. Titan's liquids: exotic behavior and its implications on global fluid circulation. Icarus 250, 64–75.
Teanby, N.A., Irwin, P.G.J., de Kok, R., 2010. Compositional evidence for Titan's stratospheric tilt. Planet. Space Sci. 58, 792–800.
Thissen, R., Vuitton, V., Lavvas, P., Lemaire, J., Dehon, C., Dutuit, O., Smith, M.A., Turchini, S., Catone, D., Yelle, R.V., Pernot, P., Somogyi, Á., Coreno, M., 2009. Laboratory studies of molecular growth in the Titan ionosphere. J. Phys. Chem. 113, 11211–11220.
Tobie, G., Lunine, J.I., Sotin, C., 2006. Episodic outgassing as the origin of atmospheric methane on Titan. Nature 440, 61–64.
Tokano, T., 2008. Dune-forming winds on Titan and the influence of topography. Icarus 194, 243–262.
Tokano, T., 2009. Impact of seas/lakes on polar meteorology of Titan: simulation by a coupled GCM-Sea model. Icarus 204.
Tokano, T., 2010. Westward rotation of the atmospheric angular momentum vector of Titan by thermal tides. Planet. Space Sci. 58, 814–829.
Tokano, T., 2011. Precipitation climatology on Titan. Science 331, 1393–1394.
Tokano, T., 2013. Are tropical cyclones possible over Titan's polar seas? Icarus 223.
Tokano, T., et al., 2001. Three-dimensional modeling of the tropospheric methane cycle on Titan. Icarus 153, 130–147.
Tomasko, M.G., Smith, P.H., 1982. Photometry and polarimetry of Titan - Pioneer 11 observations and their implications for aerosol properties. Icarus 51, 65–95. https://doi.org/10.1016/0019-1035(82)90030-6.
Tomasko, M.G., Doose, L., Engel, S., Dafoe, L.E., West, R., Lemmon, M., Karkoschka, E., See, C., 2008. A model of Titan's aerosols based on measurements made inside the atmosphere. Planet. Space Sci. 56, 669–707. https://doi.org/10.1016/j.pss.2007.11.019.
Tomasko, M.G., Doose, L.R., Moe, L.E., See, C., 2009. Limits on the size of aerosols from measurements of linear polarization in Titan's atmosphere. Icarus 204, 271–283. https://doi.org/10.1016/j.icarus.2009.05.034.
Toon, O.B., McKay, C.P., Courtin, R., Ackerman, T.P., 1988. Methane rain on Titan. Icarus 75, 255–284, 1988.
Turtle, E.P., Perry, J.E., McEwen, A.S., Del Genio, A.D., Barbara, J., West, R.A., Dawson, D.D., Porco, C.C., 2009. Cassini imaging of Titan's high-latitude lakes, clouds, and south-polar surface changes. Geophys. Res. Lett. 36. L02204.
Turtle, E.P., Del Genio, A.D., Barbara, J.M., Perry, J.E., Schaller, E.L., McEwen, A.S., West, R.A., Ray, T.L., 2011a. Seasonal changes in Titan's meteorology. Geophys. Res. Lett. 38 https://doi.org/10.1029/2010GL046266. L03203.
Turtle, E.P., Perry, J.E., Hayes, A.G., Lorenz, R.D., Barnes, J.W., McEwen, A.S., West, R.A., Del Genio, A.D., Barbara, J.M., Lunine, J.I., Schaller, E.L., Ray, T.L., Lopes, R.M.C., Stofan, E.R., 2011b. Rapid and extensive surface changes near Titan's equator:

evidence of April showers. Science 331, 1414–1417. https://doi.org/10.1126/science.1201063.
Turtle, E.P., Perry, J.E., Hayes, A.G., McEwen, A.S., 2011c. Shoreline retreat at Titan's Ontario Lacus and Arrakis Planitia from Cassini Imaging Science Subsystem observations. Icarus 212, 957–959. https://doi.org/10.1016/j.icarus.2011.02.005.
Turtle, E.P., Barnes, J.W., Perry, J., Barbara, J., Hayes, A., Corlies, P., Kelland, J., West, R.A., Del Genio, A.D., Soderblom, J.M., McEwen, A.S., Sotin, C., 2016. Cassini ISS and VIMS observations of Titan's north polar region during the T120 and T121 flybys: the Curious Case of the Clouds. Fall Meeting AGU. P33F-05.
Turtle, E.P., Perry, J.E., Barbara, J.M., West, R.A., Del Genio, A.D., McEwen, A.S., 2017. Seasonal Evolution in the Behavior of Titan's Clouds from Cassini ISS, 2004–2017. EPSC.
Turtle, E.P., Perry, J.E., Barbara, J.M., Del Genio, A.D., Sotin, C., Rodriguez, S., Lora, J.M., Faulk, S., West, R.A., Karkoschka, E., McEwen, A.S., Mastrogiuseppe, M., Hofgartner, J.D., Corlies, P., Kelland, J., Hayes, A.G., Pitesky, J., Ray, T.L., 2018. Titan insights during the final year of the Cassini mission. LPSC 49, 1656.
Veverka, J., 1973. Titan - polarimetric evidence for an optically thick atmosphere. Icarus 18, 657–660. https://doi.org/10.1016/0019-1035(73)90069-9.
Vinatier, S., Bézard, B., de Kok, R., Anderson, C.M., Samuelson, R.E., Nixon, C.A., Mamoutkine, A., Carlson, R.C., Jennings, D.E., Guandique, E.A., Bjoraker, G.L., M. Flasar, F., Kunde, V.G., 2010. Analysis of Cassini/CIRS limb spectra of Titan acquired during the nominal mission II: aerosol extinction profiles in the 600-1420 cm^{-1} spectral range. Icarus 210, 852–866.
Vixie, Graham, Barnes, Jason W., Jackson, Brian, Rodriguez, Sébastien, Le Mouélic, Stéphane, Sotin, Christophe, MacKenzie, Shannon, Wilson, Paul, 2015. Possible temperate lakes on Titan. Icarus 257, 313–323.
Volkov, A.N., Johnson, R.E., Tucker, O.J., Erwin, J.T., 2011. Thermally driven atmospheric escape: transition from hydrodynamic to Jeans escape. Astrophys. J. Lett. 729, L24. https://doi.org/10.1088/2041-8205/729/2/L24. Mar.
Vuitton, V., Yelle, R.V., McEwan, M.J., 2007. Ion chemistry and N-containing molecules in Titan's upper atmosphere. Icarus 191, 722–742.
Vuitton, V., Yelle, R.V., Cui, J., 2008. Formation and distribution of benzene on Titan. J. Geophys. Res 113, E05007.
Vuitton, V., Lavvas, P., Yelle, R.V., Galand, M., Wellbrock, A., Lewis, G.R., Coates, A.J., Wahlund, J.-E., 2009. Negative ion chemistry in Titan's upper atmosphere. Planet. Space Sci. 57, 1558–1572.
Vuitton, V., Yelle, R.V., Lavvas, P., Klippenstein, S.J., 2012. Rapid association reactions at low pressure: impact on the formation of hydrocarbons on Titan. Astrophys. J. 744, 11.
Vuitton, V., Yelle, R.V., Klippenstein, S.J., Hörst, S.M., Lavvas, P., 2018. Simulating the formation of organic species in the atmosphere of Titan with a coupled ion-neutral model. Icarus. Submitted.
Waite Jr., J.H., Niemann, H.B., Yelle, R.V., Kasprzak, W.T., Cravens, T.E., Luhmann, J.G., McNutt Jr., R.L., Ip, W.-H., Gell, D., De La Haye, V., Müller-Wodarg, I.C.F., Magee, B., Borggren, N., Ledvina, S.A., Fletcher, G.G., Walter, E.M., Miller, R., Scherer, S., Thorpe, R.L., Xu, J., Block, B.P., Arnett, K., 2005. Ion Neutral Mass Spectrometer results from the first flyby of Titan. Science 308, 982–986.
Waite Jr., J.H., Lewis, W.S., Kasprzak, W.T., Anicich, V.G., Block, B.P., Cravens, T.E., Fletcher, G.G., Ip, W.-H., Luhmann, J.G., McNutt, R.L., Niemann, H.B., Parejko, J.K., Richards, J.E., Thorpe, R.L., Walter, E.M., Yelle, R.V., 2006. Cassini Ion and Neutral Mass Spectrometer: Enceladus plume composition and structure. Science 311 (5766), 1419–1422.
Waite Jr., J.H., Young, D.T., Cravens, T.E., Coates, A.J., Crary, F.J., Magee, B., Westlake, J., 2007. The process of tholin formation in Titan's upper atmosphere. Science 316, 870–875. https://doi.org/10.1126/science.1139727.
Waite Jr., J.H., et al., 2009. Liquid water on Enceladus from observations of ammonia and ^{40}Ar in the plume. Nature 460 (7254), 487–490. https://doi.org/10.1038/nature08153.
Wall, S.D., Lopes, R.M., Stofan, E.R., Wood, C.A., Radebaugh, J.L., Stiles, B.W., Nelson, R.M., Kamp, L.W., Janssen, M.A., Lorenz, R.L., Lunine, J.I., Farr, T.G., Mitri, G., Paillou, P., Paganelli, F., Mitchell, K.L., 2009. Cassini RADAR images at Hotei Arcus and western Xanadu, Titan: evidence for recent cryovolcanic activity. Geophys. Res. Lett. 36. L04203.
Wall, S., Hayes, A., Bristow, C., Lorenz, R., Stofan, E., et al., 2010. Active shoreline of Ontario Lacus, Titan: a morphological study of the lake and its surroundings. Geophys. Res. Lett. 37.
West, R.A., Lane, A.L., Hart, H., Simmons, K.E., Hord, C.W., Coffeen, D.L., Esposito, L.W., Sato, M., Pomphrey, R.B., 1983. Voyager 2 photopolarimeter observations of Titan. J. Geophys. Res. 88, 8699–8708.
West, Robert A., Balloch, Jonathan, Dumont, Philip, Lavvas, Panayotis, Lorenz, Ralph, Rannou, Pascal, Ray, Trina, Turtle, Elizabeth P., 2011. The evolution of Titan's detached haze layer near equinox in 2009. Geophys. Res. Lett. 38 https://doi.org/10.1029/2011GL046843. L06204.
West, R.A., Del Genio, A.D., Barbara, J.M., Toledo, D., Lavvas, P., Rannou, P., Turtle, E.P., Perry, J., 2016. Cassini Imaging Science Subsystem observations of Titan's south polar cloud. Icarus 270, 399–408. https://doi.org/10.1016/j.icarus.2014.11.038.
West, R.A., Seignovert, B., Rannou, P., Dumont, P., Turtle, E.P., Perry, J., Roy, M., Ovanessian, A., 2017. Titan's Detached Haze: seasonal Cycle submitted.
Wong, M.L., Yung, Y.L., Gladstone, G.R., 2015. Pluto's implications for a snowball Titan. Icarus 246 (2015), 192–196.
Wood, C.A., Lorenz, R., Kirk, R., Lopes, R., Mitchell, K., Stofan, E., Cassini RADAR Team, 2010. Impact craters on Titan. Icarus 206, 334–344.
Yelle, R.V., Borggren, N., de la Haye, V., Kasprzak, W.T., Niemann, H.B., Müller-Wodarg, I., Waite Jr., J.H., 2006. The vertical structure of Titan's upper atmosphere from Cassini Ion Neutral Mass Spectrometer measurements. Icarus 182, 567–576.
Yelle, R.V., Cui, J., Muller-Wodarg, I.C.F., 2008. Methane escape from Titan's atmosphere. J. Geophys. Res. 113, E10003.
Yelle, R.V., Vuitton, V., Lavvas, P., Klippenstein, S.J., Smith, M.A., Hörst, S.M., Cui, J., 2010. Formation of NH_3 and CH_2NH in Titan's upper atmosphere. Faraday Discuss 147, 31–49.
Yung, Y.L., Allen, M.A., Pinto, J.P., 1984. Photochemistry of the atmosphere of Titan: comparison between models and observations. Astrophys. J. Supp. 55, 465–506.
Zhang, X., Strobel, D.F., Imanaka, H., 2017. Haze heats Pluto's atmosphere yet explains its cold temperature. Nature 551, 352–355.